Universität Rostock
Mathematisch-Naturwissenschaftliche Fakultät
Institut für Biowissenschaften

Institut für Ostseeforschung Warnemünde

Effects of the Mekong River on abundance and N_2-fixation rates of cyanobacteria in the South China Sea

Diplomarbeit

von

Julia Große

Oktober 2007

Gutachter

Dr. habil. Maren Voß

Prof. Dr. Bodo von Bodungen

Abbreviations

C	carbon
Chl-a	chlorophyll-a
CTD	Conductivity-Temperature-Density
DFG	Deutsche Forschungsgesellschaft
F_0	fluorescence before acidification
F_a	fluorescence after acidification
F/S	Forschungsschiff (research vessel)
GF/F	glass fiber filter
IRMS	isotopic ratio mass spectrometer
max.	maximum
M/V	motor vessel
n	number of events
N	nitrogen
nifH	nitrogenase gene
NO_2	nitrite
NO_3	nitrate
n.s.	not significant
p	significance
P	phosphosus
PEB	phycoerythribilin
PO_4	phosphate
POC	particulate organic carbon
PON	particulate organic nitrogen
PUB	phycourobilin
PSU	practical salinity unit
R^2	correlation factor
sd	standard diviation
Si	silicate
SCS	South China Sea

Index

1 Summary

The influence of the Mekong River discharge (South China Sea) was investigated during its lowest annual outflow in April 2007. The river plays an essential role in providing nutrients for the adjacent sea all year long. The effects of salinity (15-33 PSU) and nutrient gradients (NO_3, PO_4, Si) on nitrogen fixation (< and >10 µm) and phytoplankton community structure were examined.

High nitrogen fixation rates were detected along these gradients with rates ranging from 0.08 to 14.41 nmol N l^{-1} h^{-1} (<10 µm fraction) and 0.03 to 15.03 nmol N l^{-1} h^{-1} (>10 µm fraction). Overall, it contributed 6.8 – 163.3 % to the N-demand of primary production.

Altogether, a clear shift was observed in the composition of phytoplankton (>10 µm) from diatom dominated towards filamentous cyanobacteria. Inside the river plume *Chaetoceros*, *Rhizosolenia* and *Hemiaulus* dominated and diatom/cyanobacteria associations were considered to be responsible for the N_2-fixation. Further offshore, at stations with low nutrient concentrations, *Trichodesmium* accounted for the N_2-fixation. In the other size fraction (<10 µm), unicellular cyanobacteria were dominant and their abundance increased with distance to the coast. At the same time the number of eukaryotic algae decreased. Unfortunately, the organisms responsible for N_2-fixation were not clearly identified by flow-cytometry. Hence, heterotrophic bacteria might have also added to nitrogen fixation.

The measurements indicate that the Mekong River plume sets favorable environmental conditions for diatom/cyanobacteria associations nearshore and fosters nitrogen fixation in both size fractions. Furthermore, the investigation revealed that nitrogen fixation is also achievable in waters with high NO_3-concentrations.

Phycoerythrin was not observed at stations closest to the coast and was difficult to detect at low concentrations. Nevertheless, the <10µm fraction gave good spectra at most stations. Based on the cytometric counts these spectra were mixed signals and an established relationship between chlorophyll-a and phycoerythrin (<10µm) gave evidence that cyanobacteria <10 µm were the dominating organisms in the phytoplankton community. Besides, determination of species with the spectra from conducted net-tows identified *Trichodesmium thiebautii* which agreed with microscopic phytoplankton counts. The two spectra from *Oscillatoria* sp. showed typical peaks at 503 nm and 555 nm. However, there was no established relationship between phycoerythrin and nitrogen fixation.

Zusammenfassung

Der Einfluss des Mekongs auf das Südchinesische Meer wurde zur Zeit seines geringsten Abflusses im April 2007 untersucht. Da der Fluss ganzjährig als Nährstoffquelle für das angrenzendes Seegebiet dient, entstehen je nach Jahreszeit unterschiedlich starke Salzgehalts- und Nährstoffgradienten. Der Einfluss dieser Gradienten auf die Stickstofffixierungsleistung und die Zusammensetzung der Phytoplanktongemeinschaften sollte untersucht werden, wobei zwischen zwei Größenklassen unterschieden wurde (< und > 10µm).

Die gemessenen Raten der Stickstofffixierung waren hoch und lagen zwischen 0,08 – 14,41 nmol N l^{-1} h^{-1} (<10 µm) und 0.03 – 15,03 nmol N l^{-1} h^{-1} (>10 µm). Insgesamt wurde damit zwischen 6,8 und 163,3% des für die Primärproduktion benötigten Stickstoffes bereitgestellt.

Im Allgemeinen konnte eine Verlagerung der Phytoplanktongemeinschaft (>10 µm) von Diatomeen im küstennahen Bereich zu filamentösen Cyanobakterien im küstenferneren Bereichen festgestellt werden. In der Flussfahne selber dominierten die Arten *Chaetoceros*, *Rhizosolenia* und *Hemiaulus*. Dies führte zu der Annahme, dass Assoziationen aus Diatomeen und symbiotischen Cyanobakterien für die Stickstofffixierung in diesem Gebiet verantwortlich waren. Des Weiterem wird vermutet, dass in küstenferneren Gebieten die Fixierungsraten durch *Trichodesmium* erreicht wurden. In der <10 µm-Fraktion dominierten einzellige Cyanobakterien, deren Zellzahl mit Entfernung zur Küste zunahm. Im Gegensatz dazu, verringerte sich die Zellzahl der eukariotischen Algen mit wachsender Entfernung zur Küste. Leider konnte eine eindeutige Identifizierung der verantwortlichen Stickstofffixierer mit Hilfe der Flow-Cytometry nicht erfolgen. Deshalb ist es nicht ausgeschlossen, dass ein gewisser Teil der Fixierung von heterotrophen Bakterien beigesteuert wurde.

Die durchgeführten Messungen deuten jedoch darauf hin, dass die Flussfahne des Mekongs vorteilhafte Bedingungen für Assoziationen aus Diatomeen und Cyanobakterien schafft und zusätzlich Stickstofffixierung in beiden Größenklassen antreibt. Zusätzlich lassen die Messungen erkennen, dass Stickstofffixierung auch bei erhöhten Nitratkonzentrationen möglich scheint.

Phycoerythrin konnte an küstennahen Stationen nicht beobachtet werden, außerdem war es schwierig geringe Konzentrationen zu detektieren. Trotzdem konnten in der <10 µm-Fraktion ausgeprägte Spektren aufgezeichnet werden. Basierend auf den Daten der Flow-Cytometry sind diese Spektren allerdings Mischsignale verschiedener

Populationen. Ungeachtet dessen, konnte eine Beziehung zwischen dem Gesamtchlorophyllgehalt und dem Phycoerythringehalt der <10 µm Fraktion beobachtet werden, was darauf schließen lässt, das die Cyanobakterien der <10 µm Fraktion die dominierenden Organismen in der gesamten Phytoplanktongemeinschaft sind. Zusätzlich gelang die Identifizierung einzelner Arten mit Hilfe von gemessenen Spektren aus Netzhols. So konnte die Art *Trichodesmium thibautii* sowohl durch ihre spezifischen Phycoerythrineigenschaften als auch durch Planktonzählungen bestätigt werden. Für die Art *Oscillatoria* sp. konnten erstmals Spektren aufgezeichnet werden. Diese weisen charakteristische Fluorescenzmaxima bei 503 nm und 555 nm auf.

2 Introduction

The N-cycle is relatively more complex compared to other biogeochemical cycles. It contains numerous forms of nitrogenous compounds that appear in different phases: gaseous, dissolved, particulate, organic and inorganic. The transformations of N-species into one another occur only under specific conditions and are accomplished primarily by microbes. Combined nitrogen is expected to be limiting in most ocean surface regions and presents a major control on primary production and carbon export (Falkowski, 1997). Through the reduction of NO_3 and NO_2 to N_2 (denitrification) an amount of at least 400 Tg N a^{-1} (Codespoti, 2007) of nitrogenous nutrients is withdrawn from the ocean. This shortcoming has to be balanced by an opposite process that fixes N_2. Nitrogen gas is the dominant component in the N-cycle, but unfortunately, it is largely unavailable and only selected groups of bacteria, including cyanobacteria and *Archaea* are capable of N_2-fixation. The process of nitrogen fixation requires a special enzyme, nitrogenase, which is able to convert N_2 to ammonium. The ammonium is then incorporated into amino acids and can enter the food web through the N_2-fixing organism itself or as excreted dissolved organic nitrogen.

The contribution of marine N_2-fixation to the global N-budget seems to play a major role especially in the tropical and subtropical regions (Karl et al., 2002). So far, estimations on global ocean N_2-fixation range between 100 - 200 Tg N a^{-1} (e.g. Gruber and Sarmiento, 2002; Codespoti, 2007). Compared to the amount of N_2 released through denitrification a deficit of ~200 Tg N a^{-1} (Codespoti, 2007) emerges. Consequently, nitrogen fixation might be more important than previously assumed.

In oligotrophic waters of tropical and subtropical areas the filamentous cyanobacterium *Trichodesmium* was thought to be the most important diazotroph because of its ability to form extensive blooms (Capone et al., 1997, 1998). It mainly resides in the upper layer of the euphotic zone and demonstrates repressed N_2-fixation when combined nitrogen is available at concentrations >1 µmol/l (Holl and Montoya, 2005).

Heterocystous cyanobacteria are common in coastal and shelf waters (Marshall, 1981) including diazotrophs that are known to establish symbioses with diatoms. The two species *Richelia intracellularis* and *Calothrix rhizosoleniae* are morphologically very similar and can be found as extracellular and intracellular symbionts in various diatom species (Villareal, 1992; Janson et al., 1999; Carpenter 2002). However, *Richelia* is observed as a free-living organism as well (Gómez et al., 2005), but it lacks of gas

vesicles, and therefore profits from the buoyancy of its host diatom (Janson et al, 1995). It is also proofed that *Richelia* is able to supply all the nitrogen required by their host-diatom (Carpenter, 2002). This enables the diatoms to build up extensive blooms in river plume areas (Carpenter et al., 1999).

Recently, the attention included to small diazotrophs (<10µm), comprising coccoid cyanobacteria and proteobacteria, that seem to play a significant role in fostering new production in the euphotic zone (Zehr et al. 2001; Montoya et al., 2004). At the moment the determination of unicellular cyanobacteria is based on the expressed *nifH*-genes and recently the number of *nifH*- gene copies per samples was used to give cell specific nitrogen fixation rates (Zehr et al., 2007) The distribution of unicellular cyanobacteria within the water column applies to be more uniform then that of *Trichodesmium* and they are also found in waters that present significant concentrations of NO_3 (Langlois et al, 2005).

The importance of unicellular cyanobacteria of the size ≤ 2 µm as primary producers was already recognized in the 1970s (Azam et al., 1983). They occur in all but the polar seas and can reach abundances of 10^8 cells/l in warm waters (Campbell and Vaulot, 1993). Specifically dominant is the genus *Prochlorococcus* that exhibits its highest abundance in oligotrophic ocean areas (Chisholm et al., 1988; Campbell and Vaulot, 1993). However, it is little known about picoplankton in coastal and river waters.

Nevertheless, the chemical parameters such as nutrient and trace metal content as well as the discharge volume and sediment load are well studied for tropical rivers (Nittrouer et al., 1995). However, knowledge of the bioavailability and their influence on biological processes such as primary production, bacterial activity, nitrogen fixation, etc. is less well studied. A few river plumes have been investigated so far and especially the Amazon River is well studied regarding phytoplankton composition and diazotrophic activity (Carpenter et al., 1999; Capone et al., 2005; Foster et al., 2007). Furthermore, it is assumed that nitrogen fixation off the coast of Africa (Voss et al., 2004) was partly driven by the influence of river water (Voss, pers. comm.). Recent studies in the South China Sea (SCS) suggest that the Mekong River stimulates N_2-fixation during the south-west monsoon (Voss et al., 2006).

This diploma thesis investigates the direct effect of the Mekong River on the amount of N_2-fixation in the South China Sea during an intermonsoon. The freshwater discharge of the Mekong River is relatively low (2.100m^3/s – 40.000 m^3/s) compared to the Amazon River (34.000 m^3/s – 121.000 m^3/s; http://encarta.msn.com/encyclopedia_761571466/

Amazon_(river).html), but the river water also induces steep gradients in salinity and nutrient concentrations. Additionally, the Mekong River area is influenced by two overlapping tides that induce constantly changing currents.

Another main focus lies on changes in community structure along the salinity and nutrient gradients. Hereby, special attention is put on the proportion of cyanobacteria on the overall phytoplankton community and the changes in nitrogen fixation rates. Furthermore, this study is an attempt to clarify the importance of filamentous cyanobacteria, diatom/cyanobacterial-associations, and unicellular cyanobacteria.

The work presented here is part of the DFG-funded project “Pelagic processes and nitrogen cycle in coastal waters off southern central Vietnam”. The project is carried out in close collaboration between the Institute of Baltic Sea Research, Germany and Institute of Oceanography in Nha Trang, Vietnam. The project specifically focuses on the role of Mekong water on primary production and nitrogen dynamics, especially on the uptake of different nitrogen species.

3 Methods

3.1 Area of investigation

The South China Sea (SCS) is a marginal sea of the northern Pacific Ocean. It extends from the equator to 23°N and from 99°E to 121°E. The greatest depths are located in the central basin and reach more than 5000m. The basin is bordered by two shelf regions, both no more than 200 m in depth (Dippner, 2007). In the south it is the Sunda Shelf with a connection to the Golf of Thailand. This shallow region has limited water exchange with the Indian Ocean and the Java Sea through the Malacca Strait and the Karimata Strait, respectively. A narrow band of continental shelf with a rim, only 35 km away from the coast, connects the Sunda Shelf with the Golf of Tonkin, located off the coast of northern Vietnam. Here, the SCS connects with the East China Sea and the Pacific Ocean and exchanges the main amount of water via the Taiwan Strait and the Luzon Strait where salty and nutrient poor water from the Kurishio Current enters (Chen, 2001).

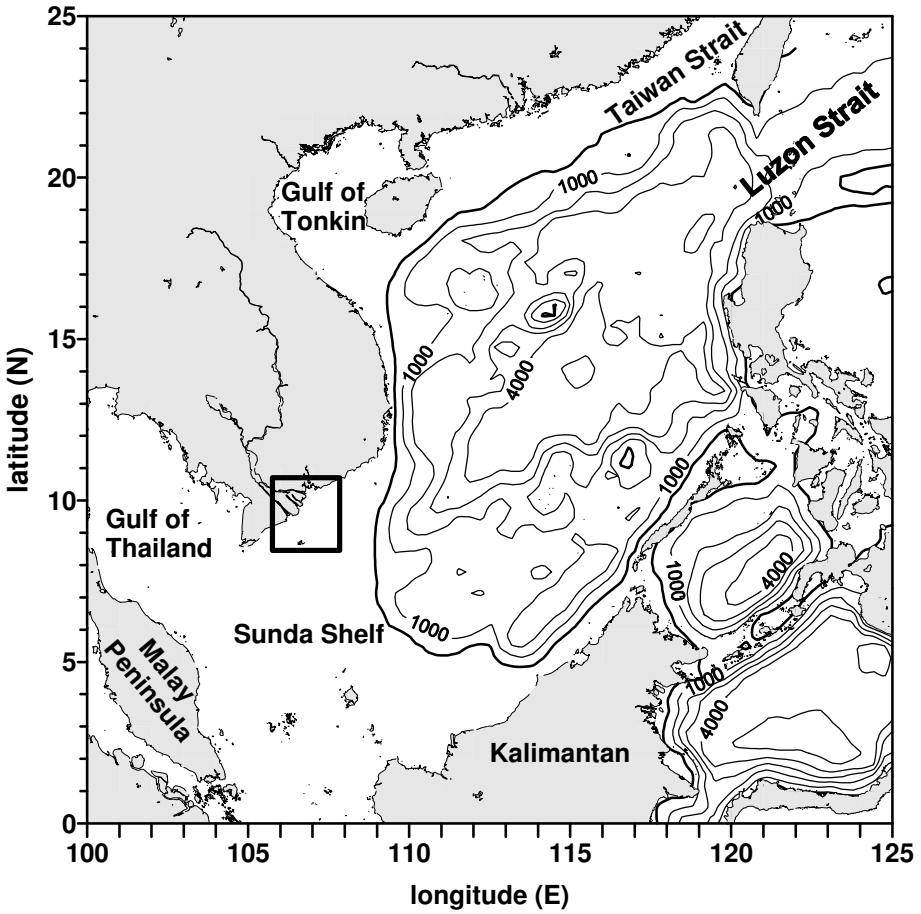

Fig.1: Map of the South China Sea. The rectangle marks the investigation area from April 2007. (after Dippner et al., 2007)

Laying in the East-Asian-Monsoon region the SCS is affected by seasonally reversing monsoon winds. The annual cycle of wind stress fields is the main driving force for the seasonal changes in surface circulation (Hellerman and Rosenstein, 1983).

The northeast monsoon appears between November and March affecting the whole SCS. The prevailing winds have an average velocity of 9 m/s and induce a cyclonic gyre. In contrast, the southwest monsoon lasts from June to September when prevalent winds are less strong with an approximate wind speed of 6 m/s. They generate the formation of an anticyclonic gyre in the southern basin while a smaller cyclonic gyre still persists in the northern part of the SCS. This results in a summer southeast offshore current (Fang, 1998) and induces coastal upwelling at ~11-12°N latitude (Dippner et al., 2007). The intermonsoon marks a sharp transitions between the monsoon seasons and emerge in April/May as well as in October/early November (Fang et al., 2002).

In the south of Vietnam the monsoon winds affect the flow-direction of the Mekong River plume. During the summer large amounts of river water are transported north-east along the coast. In winter, most of the river water is advected near the shore in a south-east direction (Hu et al., 2000).

The Mekong River has its source in the Tibetan mountains and flows down the Indochina Peninsula before it empties into the South China Sea. With a length of 4.350 km and a water discharge volume of 470 km^3 annually it is one of the largest rivers in the world (Saito, 2001). The water is distributed by three major channels, the two Mekong Rivers and the Bassac River. The river run-off also varies seasonally, between 2.100 m^3/s in April and 40.000 m^3/s in September/October (Hoa et al., 2007).

Furthermore, the water transports enormous amounts of sediment (160 million t/a; Milliman et al., 1995) and forms one of the largest deltas in Southeast Asia. The precipitating sediment moves the shoreline seawards and extends the delta approximately 9 km^2/a (Saito, 2001).

The region is affected by two overlapping tidal sources, a 3.5 m semidiurnal tide from the South China Sea and a 0.8-1 m diurnal tide from the Gulf of Thailand (Hoa et al, 2007).

The investigation area was located in the Mekong River discharge area (Fig.:1). A cruise was conducted from April 15 to 20, 2007 onboard the M/V *BTh-0666 KN*, a Vietnamese fishing vessel. It started in Phan Thiet and ended in Vung Tau. Both cities are located north of the Mekong Delta. Three transects were investigated, each starting in one of the main distribution channels of the Mekong River and reaching out into the

SCS. Samples were taken at a total of 25 stations, including two time-series stations that were sampled 24 hours and 14 hours, respectively to study day-night changes as well as tidal cycles. At all stations the water was taken with a Niskin-bottle (10 liter) or a bucket from the upper two meter of the water column.

A year earlier a cruise on F/S SONNE took place from April 12 to 21, 2006. Sampled stations in the Mekong estuary will be evaluated and discussed in this work as well (Fig. 2).

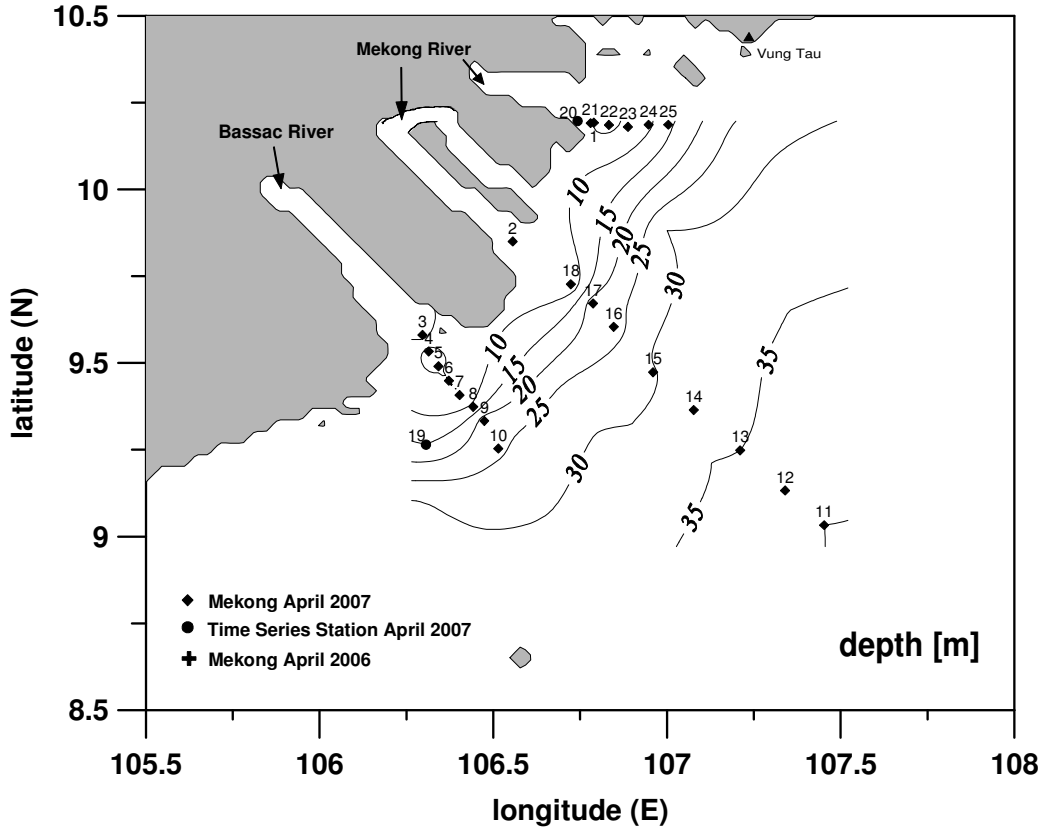

Fig. 2: Station map with stations from Mekong cruises April 2006 and 2007; isolines give the depth in meter

3.2 Nutrients

For nutrient measurements the colorimetric determination of nitrite, nitrate, phosphate and silicate after Grasshoff (1983) was applied. Nitrate was reduced to nitrite by copper-plated cadmium columns. The nitrite reacts with an aromatic amines and forms a red aco-dye. A concentration range between 0-40 µmol/l can be measured without a sample dilution. The precision of this method is ± 0.5 µmol/l.

The determination of phosphate and silicate is based upon the formation of molybdenium blue. Hereby, the reaction to heteropolymolybdenium- phosphoric acid occurs at a pH below 1. This method is suited for a concentration range between 0-25 µmol/l with an precision of 0.03 µmol/l. Silicon-molybdenium acid forms at a pH rage between 1.4 and 2.6. Here the precision is 0.1 µmol/l in the detection range between 0-200µmol/l.

3.3 Particulate Silicate

Dependent on the water turbidity the maximum possible amount of water (200 and 2000 ml) was filtered on cellulose-acetate filters (SATORIUS) with a pore size of 0.45 µm. Afterwards, those filters were dried (at 60°C for 48 h) and shipped to the institute for further analysis.

In the laboratory the filters were added to polycarbonate bottles containing 25 ml of 0.1 µmol/l sodium hydroxide solution that was already heated up to 85°C. The extraction continued for two hours in a shaking bath with a temperature constant at 85°C. After neutralization of the sodium hydroxide with 0.1µmol/l sulfuric acid the determination of particulate silicate followed the description of Grasshoff (1983).

3.4 Chlorophyll

Dependent on the water turbidity the maximum possible volume of water (200 and 2000 ml) was filtered on GF/F (WHATMAN) and stored deep frozen before analyzed in the laboratory. The determination of chlorophyll-a and phaeopigment took place concurrently. Therefore, the filters were extracted in 10 ml ethanol (96%) for 3 hours at room temperature while kept in the dark. The first measurement was conducted at a fluorometer (TURNER 10-AU-005) by determining the overall fluorescence (F_0). Afterwards, 100µl 1N hydrochloric acid were added to the sample, mixed and the fluorescence (F_a) was measured again. With the following equations the amounts of chlorophyll in fresh biomass as well as degraded chlorophyll were calculated after Edler (1979).

$$Chla[\mu g/l] = F_m * (F_m - 1)^{-1} * (F_0 - F_a) * K_x * V_E * V_f^{-1}$$

$$Phaeo[\mu g/l] = F_m * (F_m - 1)^{-1} * [(F_m * F_a) - F_0] * K_x * V_E * V_f^{-1}$$

Hereby, F_m is the acidification coefficient (1.9189), K_x is the linear calibration factor (1.0778), V_E is the extraction volume in ml, and V_f the filtrated volume in ml.

3.5 Rates of Nitrogen Fixation and Primary Production

3.5.1 Particulate organic nitrogen (PON) and particulate organic carbon (POC)

For the analysis of particulate organic nitrogen (PON) and particulate organic carbon (POC) surface water was taken with Niskin bottles and the maximal possible volume (300 - 2000 ml; depending on water turbidity) was filtered on pre-combusted GF/F (WHATMAN, 4 h at 500°C, 0.8 µm pore size). The filters were packed into Eppendorff cups and kept frozen until they were dried at 60°C for 48 h. In the laboratory the filters were acidified over fuming hydrochloric acid (37%) for six hours. Afterwards, the samples were dried again (40°C; 12 h), packed into tin cups and pressed into pellets before measured with a Carlo Erba elemental analyzer 1108 estimating carbon and nitrogen content. Subsequently, a Finnigan DELTA S- isotope ratio mass spectrometer (IRMS) determined the corresponding isotopic ratios ($^{15}N/^{14}N$; $^{13}C/^{12}C$). The ratio is given as the δ -value in ‰ and refers an accumulation of heavy or light isotopes (Sigman and Casciotti, 2001).

3.5.2 Nitrogen fixation measurements with the $^{15}N_2$-Tracer Method

Nitrogen fixation and primary production were measured at the same time using the high-sensitivity tracer assay for N_2-fixation as described by Montoya et al. (1996). Surface water was taken with Niskin bottles and filled into 2.3 liter Nalgene bottles (three parallels). The bottles were sealed with septum caps made of Teflon-lined butyl rubber. Subsequently, the tracer substances, $^{15}N_2$-gas (2 ml; Sercon, 99 atom%) for nitrogen fixation and 0.1 µmol/l $NaH^{13}CO_3$ solution (0.5 ml; Sigma Adrich, 98 atom%) for primary production, were added with syringes. The bottles were incubated on deck and rinsed thoroughly with seawater. During the day the incubation lasted 6 hours and incubation tubs were covered with natural density screens that allowed 50% light penetration. The light intensity simulated surface condition of mesotrophic surface waters and 10 m depths in oligothrophic waters, respectively. In the dark (night conditions) the incubation lasted 12 hours to assure a nitrogen uptake above the detection limit. The incubations started at different times of the day, so samples from different stations were exposed to different light intensities.

The incubation was stopped by filtering the bottle content. In order to achieve a separation between unicellular (<10 µm) and filamentous (>10 µm) cyanobacteria the

bottle content was passed trough a gauze (10 µm pore-size). Afterwards, the filtrate was filtered again over a pre-combusted GF/F (WHATMAN) to catch the <10 µm fraction. The material from the gauze was washed onto another GF/F (WHATMAN). The amount of water filtered per size fraction and filter depended on the amount of particulate matter suspended in the sample. Further, the samples were handled the same way as samples for PON and POC. N_2-fixation and primary production were calculated after Montoya et al. (1996).

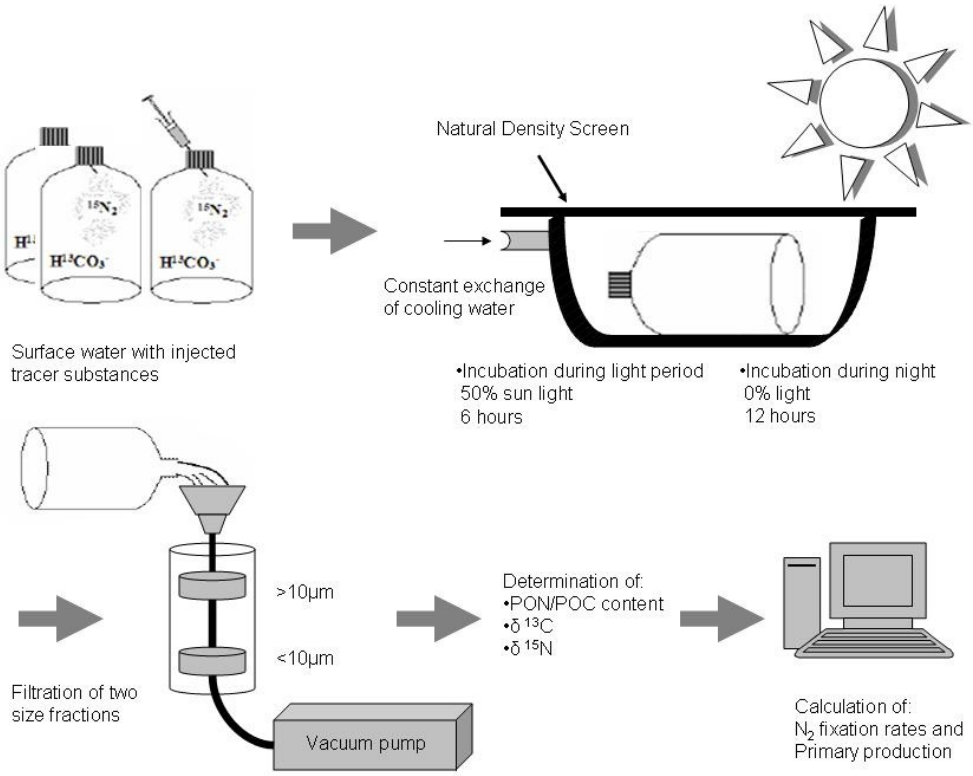

Fig. 3: Operational sequence of $^{15}N_2$- and $NaH^{13}CO_3$ experiments

3.6 Cytometry

3.6.1 Theoretical background

Flow-cytometry provides an essential tool for studies of aquatic microbial communities. Phytoplankton populations can be distinguished and enumerated by measuring different cell properties such as auto-fluorescence at different wavelengths (Campbell, 2001). The instrument used in this work was a FACSCalibur (Becton Dickinson). It consists of three components: fluids, optics and electronics for detection and data acquisition. The fluid system covers every cell individually and forces it through a pressurized fluid delivery system. Then the cell passes the focused laser beam (488 nm) within the sensing region of the flow cell. The light is scattered by the cell in the forward angle light and detected by a photodiode. Light scattered at right angles into the cell passes through a dichroic filter that splits the light into wavelengths >560nm and <560nm. Fluorescence >560 nm is subsequently split again with a 640-nm-long pass filter. The wavelength >650 nm are detected by the red fluorescence photomultiplier and refer to chlorophyll and the range of wavelengths within 560 -640 nm is detected by orange fluorescence photomultiplier which refers to phycoerythrin. Fluorescence within the range of 515-545 nm is collected by the green photomultiplier (Fig.4, Campbell, 2001).

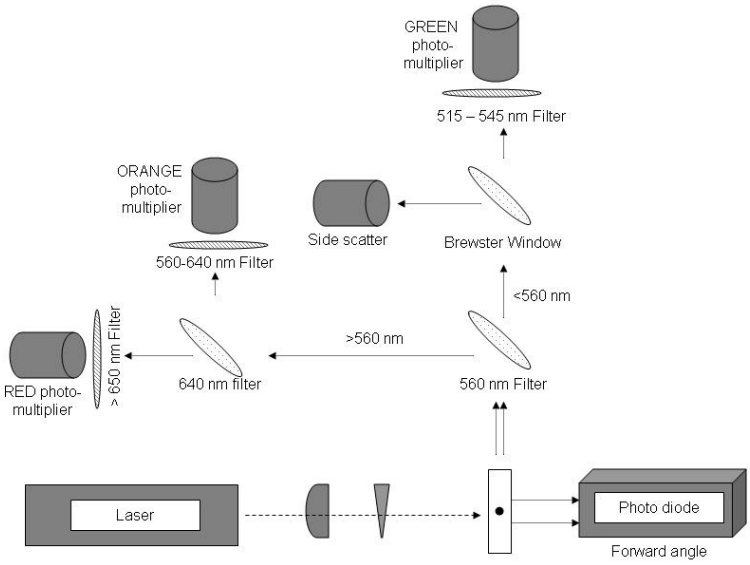

Fig.4: Standard optics layout for the FACSCalibur flow-cytometer. (Campbell, 2001)

The red and orange auto-fluorescence signals form phytoplankton as well as the side scatter signal, which is influenced by the internal cell structure, are used to determine the different phytoplankton populations. Phytoplankton does not establish green fluorescence signals. This signal however is used to evaluate bacteria abundances by treating the samples with green fluorescent DNA-dyes.
The detected signals are displayed on a computer screen and can be saved for further processing.

3.6.2 Sample collection and treatment

For cell counts 2 ml of water were pre-filtered through 10 µm-gauze and filled into cryovials (two parallels). Immediately, 20 µl of formaldehyde (35%) were added. Samples were fixed at room temperature for 10 minutes, quick frozen in liquid nitrogen and stored at -80°C until further preceded.

3.6.3 Measurements and data analysis

The samples were measured following the protocol described by Campbell (2001). Therefore, the samples were kept in a dark place to thaw. From each sample 500 µl were transferred into a sampling tube and 10 µl of calibration beads (0.95 µm) were added. Samples were run under medium flow rate (45 µl/min) for 3 minutes to acquire a moderate number of events for further interpretation. The measured parameters included forward angle light, side scatter, green, orange and red fluorescence. The stored data were further evaluated with the software Win MDI. Different populations were defined and gated by plotting the measured parameter against each other which resulted in different plots that describe different populations. For the analysis of phytoplankton the fluorescence signals red and orange as well as red and side scatter are plotted against each other.
The number of cells per population was displayed and cell numbers per milliliter were calculated with the following equation.

$$\left[cell * ml^{-1}\right] = n/(T * R) * CF * 1000\mu l * ml^{-1}$$

Hereby, n is the number of events, T the duration that the sample was analyzed (3min) and R refers to the flow rate (45µl/min). The correction factor (CF) accounts for the dilution of the original water sample through the fixation solution and the addition of

beads. In case of this investigation the CF is 0.99 for the sample fixation and 0.98 for the addition of beads (overall CF: 0.97).

3.7 Plankton counts

Phytoplankton samples were taken from the surface either with a Niskin bottle or with a bucket. A volume of 1.5 liter was preserved with 0.5ml Formaldehyde (33%) and with five to ten milliliters of Lugol solution, depending on phytoplankton abundance.
The determination and counting of phytoplankton in the size fraction >10 µm was carried out by Vietnamese researchers at the Institute of Oceanography, Nha Trang, using standard protocols after Utermöhl (1958).

3.8 Phycoerythrin

3.8.1 Sample collection and treatment

Measurements of the phycoerythrin amount were conducted using the methods of extraction and quantification described by Lantoine and Neveux (1997).
Water samples were taken from the upper 2 meters of the water column using Niskin bottles. The maximum possible amount of water (0.2 to 6.0 liters), depending on size fraction and the amount of suspended matter, was filtered on GF/F (WHATMAN). A size fractionation >10 µm and <10 µm was performed as described before. The filters were stored in liquid nitrogen.
In the laboratory the filters were cut into pieces and sonicated (twice for one minute) in 5 ml of a 50/50 mixture of glycerol and 0.1 mol/l phosphate buffer (pH 6.5) and extracted for 3 h at 4°C in a dark place. After shaking the samples intensely they were centrifuged at 4°C at 3000 rpm for 20 minutes. Thereafter, the fluorescence of the supernatant was recorded with a HITACHI 4010 spectrofluorometer applying the settings described by Lantoine and Neveux (1997). First, an excitation spectrum was run from 450 nm to 580 nm with an emission wavelength of 605 nm. Subsequently, an emission spectrum was recorded between 530 nm and 650 nm using the wavelength of the first peak for the excitation. An excitation spectrum of phycoerythrin-detection exhibits two distinct peaks that are associated with two different prosthetic groups: phycourobilin (PUB) and phycoerythrobilin (PEB) (figure 5). The ratio between PUB and PEB as well as the integrated area under the fluorescence excitation curve was used to assess the phycoerythrin concentration. The highest calculated area/l was used for

normalization. It was postulated to be one and all other phycoerythrin concentrations refer as a proportion to the highest value.

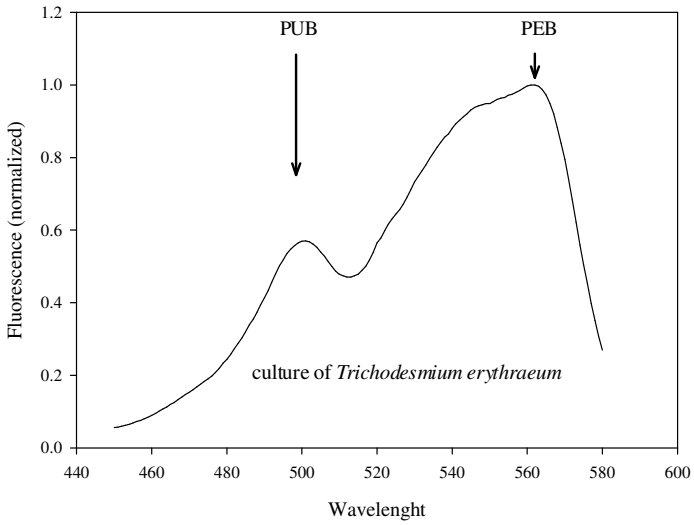

Fig. 5: Excitation spectrum of a *Trichodesmium erythraeum* culture with distinct peaks of PUB and PEB; excitation: 450nm - 580 nm, emission: 605 nm

At stations that exhibited visible amounts of filamentous cyanobacteria net tows were conducted with a 10 µm phytoplankton net. The net samples were used to record spectra from highly enriched samples.

4 Results

4.1 Surface Distribution

4.1.1 Hydrography

Three transects with a total of 25 stations have been sampled. Transect 1 in the north and transect 3 in the south had a close focus on near shore waters with distances into the sea of 29 km and 41 km, respectively. Distances between stations were approximately 5.6 km (3 nautical miles). Transect 2 (the middle transect) reached 135 km into the open SCS with a distance of 18.5 km (10 nautical miles) between stations. Its purpose was the investigation of changes in all measured parameters between eutrophic coastal waters and more oligotrophic oceanic water.

All transects started within a river arm and ran straight into the open sea (figure 6 A). Therefore, no exact distances to the coast can be given and stations 20, 2 and 3 refer as an indicator for the distance to the coast.

The surface salinity distribution demonstrated the influence of the river water (Fig. 6 A). Stations 3 and 4 had salinities below 20 PSU. A rapid increase towards 32 PSU took place within 25 km off the coast.

Temperatures were high, ranging from 29.5 °C to 31.5 °C (Fig. 6 B). No temperature gradient was observed. The highest temperatures were measured at shallow river mouth stations and on stations sampled at midday hours.

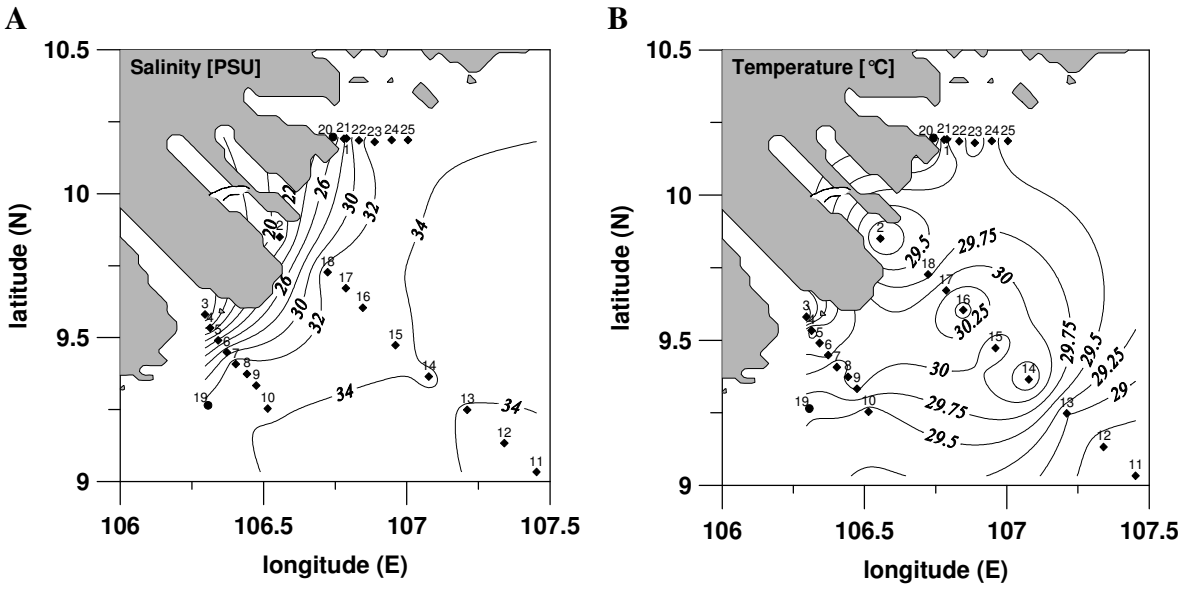

Fig. 6: Distribution of salinity (A) and temperature (B) in April 2007

The vertical salinity distribution (Fig. 7) revealed that the estuary was well mixed. The contribution of river discharge was greatest in the south (transect 3), where the salinity of "coastal stations" was lowest. The observed salinity gradient was greatest between stations 4 and 5 with a change in salinity of 1.1 PSU/km. Salinities of 33 PSU, reflecting oceanic conditions, were reached at distances approximately 25 km off the coast on transect 2 and 3, and about 10 km off the coast on transect 1.

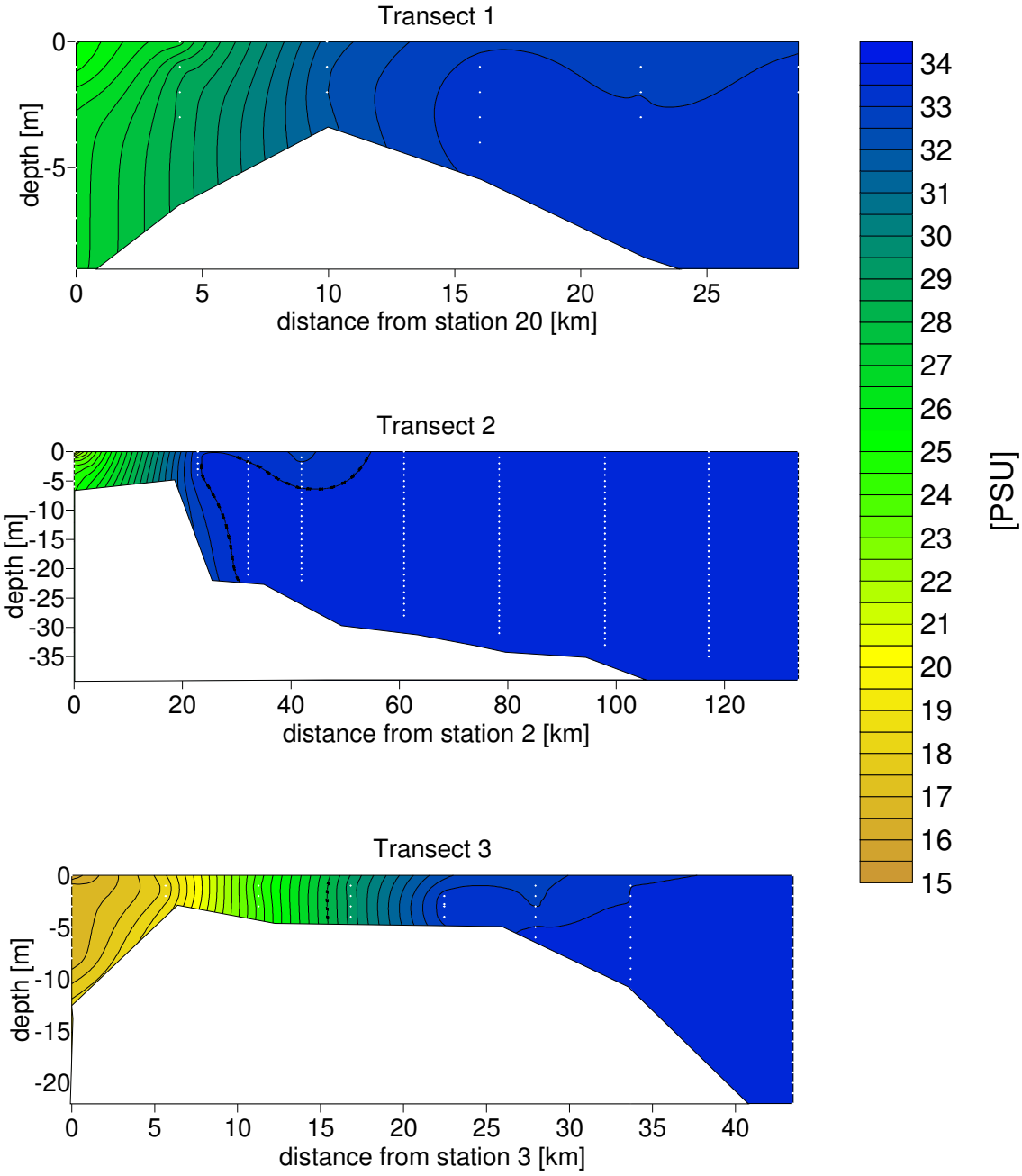

Fig. 7: Vertical salinity distribution along the sampled transects, the sampling was independent of the tides in April 2007

4.1.2 Nutrients and Chlorophyll

Stations were separated into “coastal stations”, “oceanic stations” and “intermediate stations”. The separation was based on the relationship between chlorophyll-a- and POC-concentration. This relation is displayed in figure 8 and showed three clusters. High chlorophyll-a- and POC-concentrations determined “coastal stations” and low chlorophyll-a- and POC-concentrations characterized “oceanic stations”.

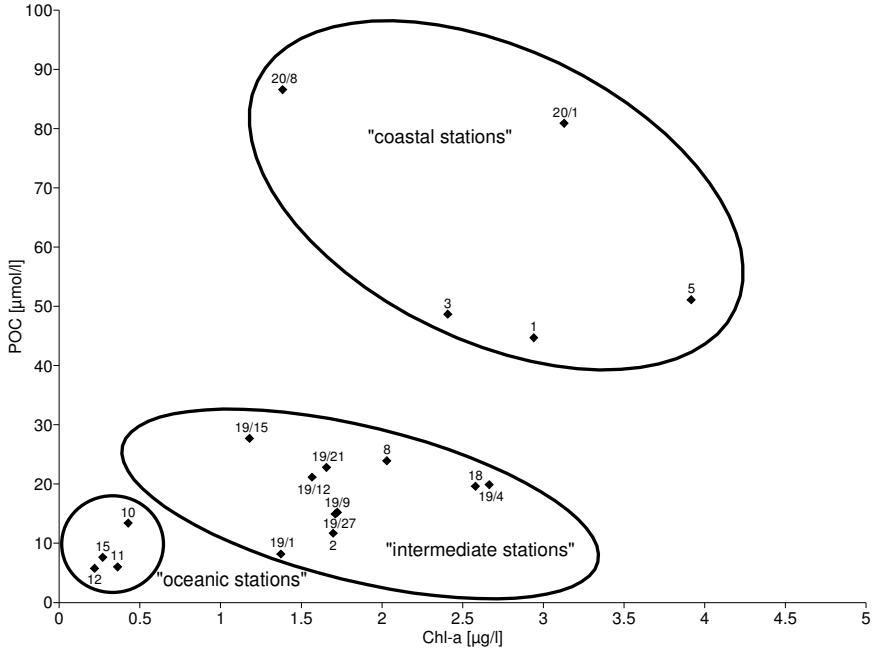

Fig.8: Classification of stations as “coastal”, “intermediate” and “oceanic”

The nutrient concentrations were highest at river mouth stations and decreased gradually with increasing distance to the coast. The water at the outermost stations (10 – 15) was nutrient depleted, regarding to NO_3 and PO_4.

Nitrate concentrations ranged from 12.9 µmol/l at station 20, 24.4µmol/l at station 2 (highest detected concentration), and 10.3µmol/l at station 3 within the river arms, and fell below detection limit at stations furthest from the coast (station 9-15) (Fig. 9 A). The same applied to phosphate concentrations. Highest values were detected within the river arms with 0.75µmol/l at station 20; 0.66µmol/l at station 2 and 0.97µmol/l at station 3 (highest measured concentration). “Oceanic stations” had values below detection limit (Fig. 9 B).

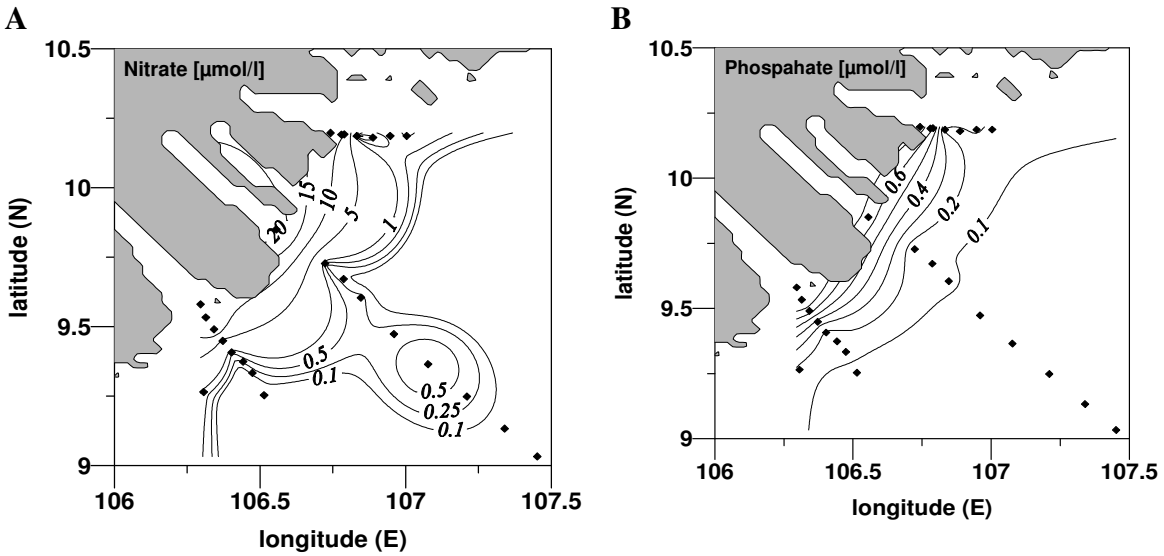

Fig. 9: Surface distribution of nitrate (A) and phosphate (B) in April 2007

River mouth stations also showed highest values of dissolved silicate with 32.9 µmol/l at station 20, 36.5 µmol/l at station 2, and 41.6 µmol/l at station 3. At station 5 an even higher value of 42.6 µmol/l was detected. Silicate concentrations decreased to about 2 µmol/l at "oceanic stations" but did not reach detection limit at any time (Fig. 10 A). Declining concentrations of dissolved silicate significantly correlated with declining concentrations of particulate silicate (Fig. 10 A and 10 B). The "oceanic stations" 10-12 obtained the lowest concentrations for particulate silicate which were just above the detection limit.

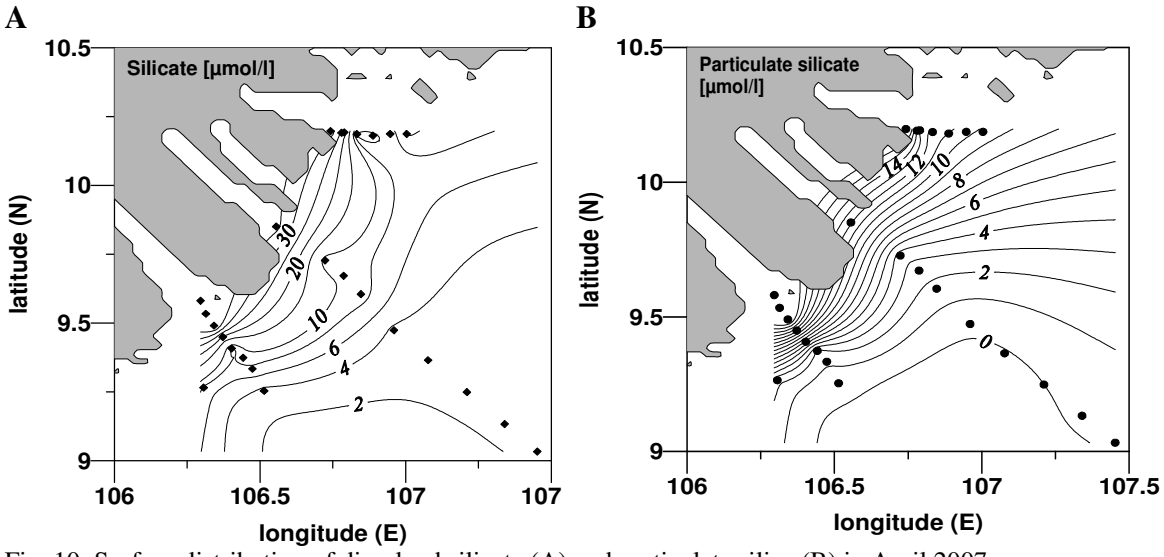

Fig. 10: Surface distribution of dissolved silicate (A) and particulate silica (B) in April 2007

The distribution of nutrients alone did not give information about which nutrient is actually limiting to the system. In figure 11 the PO_4 (A) and Si (B) values were plotted versus combined concentrations of NO_3 and NO_2. Phosphate and silicate were both remaining in small concentrations when nitrate/nitrite was depleted. With a N:P ratio >16 combined nitrogen is theoretically not limiting the system but the diagram indicates that when NO_3 + NO_2 is depleted some PO_4 is still remaining. The same picture emerged in figure 11 B, where Si was still present when NO_3 + NO_2 was depleted.

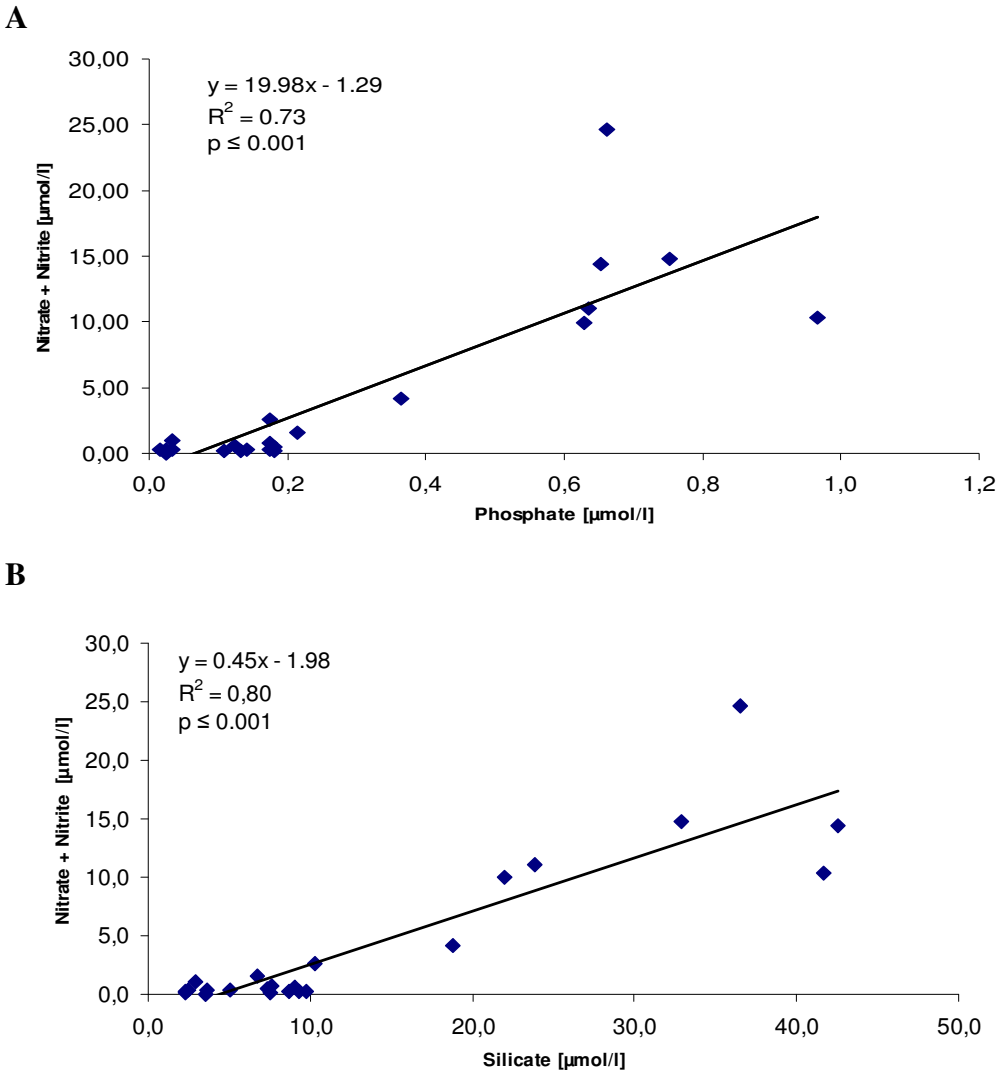

Fig. 11: Relationship between concentrations of nitrate and phosphate (A) and nitrate and silicate (B)

Plotting the measured nutrients versus the salinity can give information on the nutrient demand at different salinities. Plots for the Mekong area are shown in figures 12 A – C and revealed that PO_4 and NO_3 established a surplus at salinities between 20 and 30 PSU but at salinities >30 PSU it implied a deficit. On the other hand, a deficit of silicate was observed between 10 and 20 PSU. At salinities >20 PSU silicate-concentrations decreased gradually.

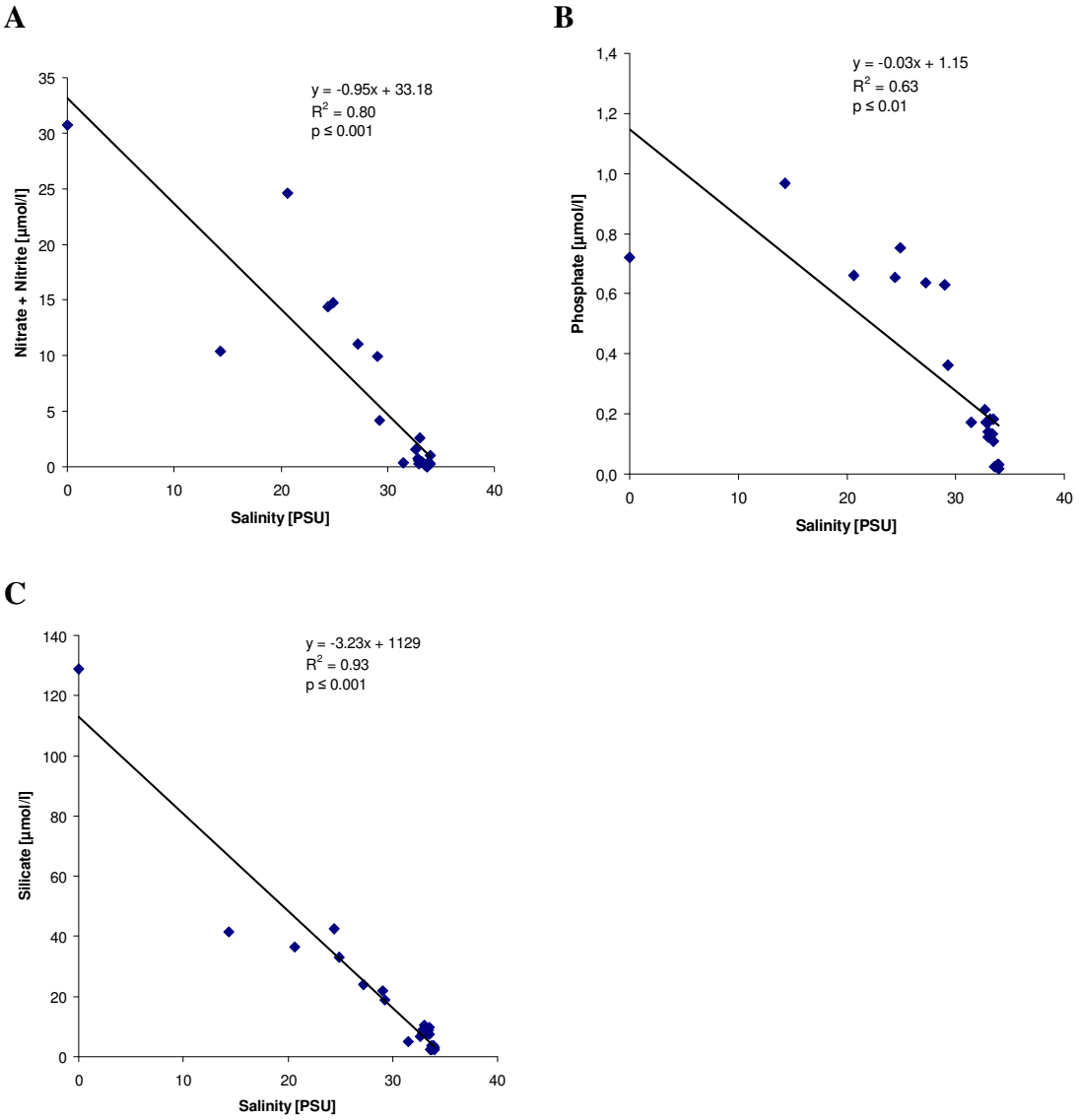

Fig. 12: Nutrient concentrations plotted over salinity: (A) NO_3 + NO_2, (B) PO_4, (C) Si. Graphs include nutrient concentrations from Mekong water of 0 PSU

The chlorophyll-a values were mapped in figure 13 and showed a decrease in concentration from “coastal” to “oceanic stations”. The degraded form of chlorophyll (phaeopigment) contributed 20-56% to the overall concentration of chlorophyll-a and phaeopigment. Phaeopigment concentrations and contributions were highest at “coastal stations”.

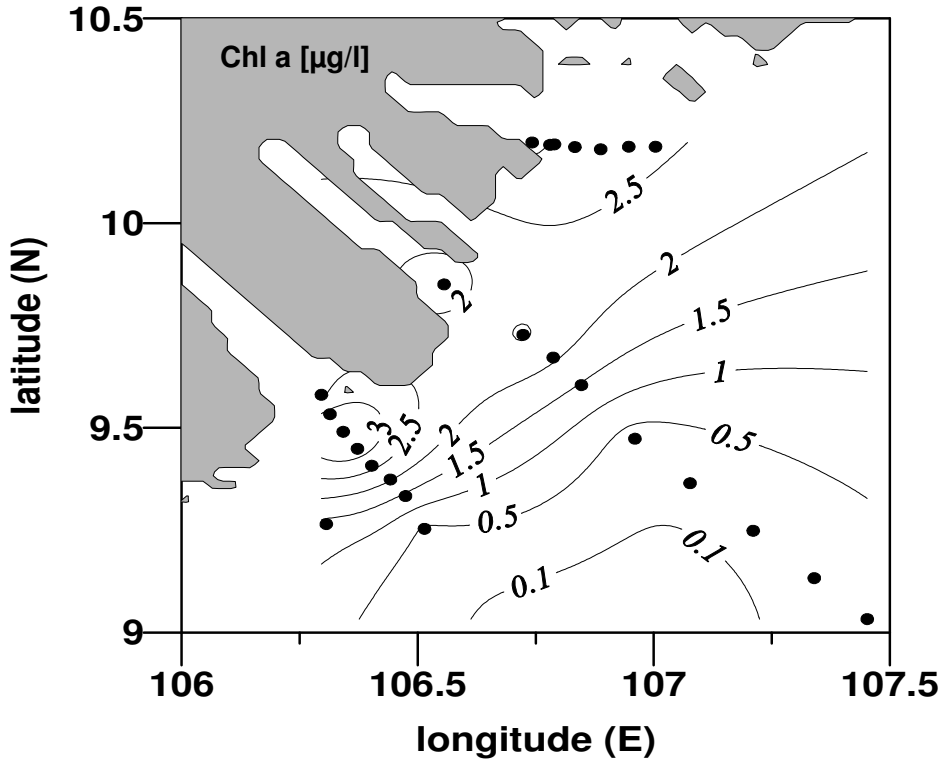

Fig. 13: Surface distribution of chlorophyll-a in April 2007

4.1.3 Nitrogen Fixation

Nitrogen fixation rates were examined at 9 stations in surface waters only (including time-series station 19; see chapter 4.2.3). The measurements included four night-incubations (including two at station 19) and 12 day-incubations (including five at station 19).

Total fixation rates were calculated by adding the rates from both size fractions. The exact measured values of all parallels can be found in the annex.

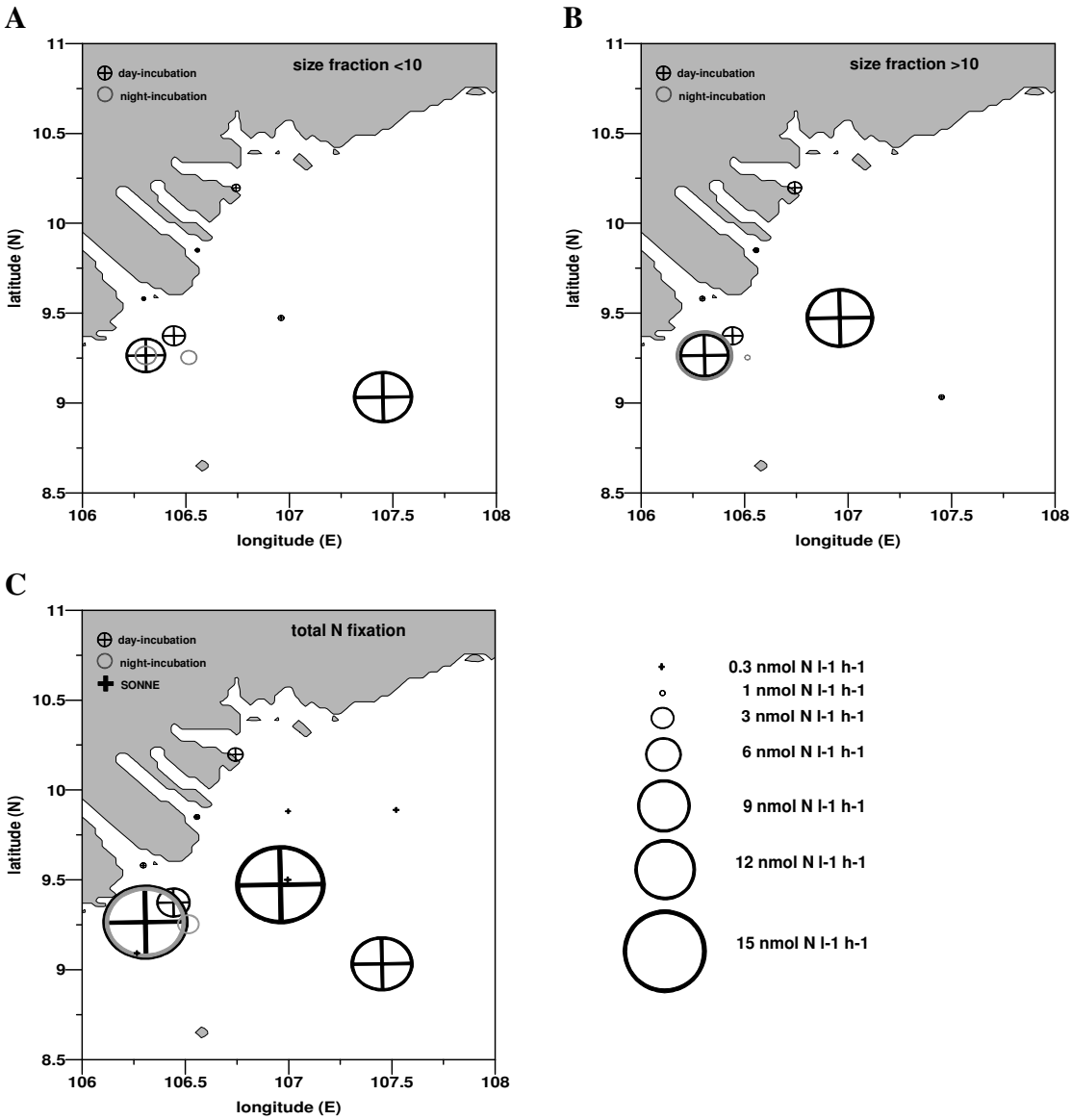

Fig. 14: Nitrogen fixation rates; within size fractions <10 µm (A), >10 µm (B) and total rates (C) from April 2006 (SONNE) and April 2007 (day-incubations/ night-incubations); values are means over parallels

Measured rates ranged from 0.03 - 15.28 nmol N l^{-1} h^{-1}. Lowest rates were found at "coastal stations" in both size fractions.

Nitrogen fixation was highest in the <10 µm fraction, except for stations 15 and 19. The < 10 µm fixation rates exceeded the >10µm fixation rates by a magnitude of ~1.5 to ~3.5. Station 11 presented an exception. There, the ratio between the size fractions <10 µm and >10 µm fraction was 20.

Low fixation rates < 1 nmol N l^{-1} h^{-1} were observed only on "coastal stations" (both size fractions) and on "oceanic stations" in the >10µm fraction during night-incubations. All other stations had rates >1.0 nmol N l^{-1} h^{-1}.

Incubations from April 2006 had N_2-fixation rates <0.3 nmol N l^{-1} h^{-1} for total fixation.

Fixation rates exhibited very significant relationships with NO_3 + NO_2, PO_4 and Si. In figure 15 N_2-fixation was plotted over the NO_3 + NO_2- concentration to show an example. Low nutrient-concentrations resulted in high N_2-fixation rates and high nutrient-concentrations resulted in low N_2-fixation rates.

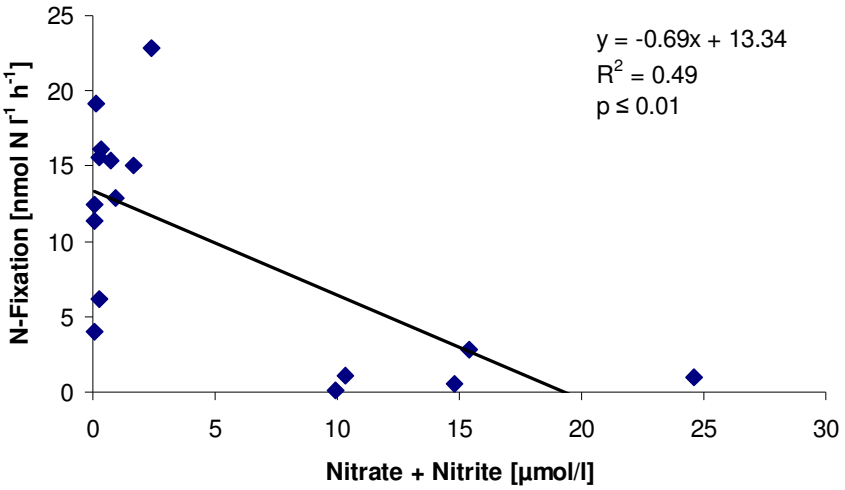

Fig. 15: Relationship between NO_3 + NO_2 concentrations and total N_2-fixation

Concurrently, primary production was measured. At "coastal stations" (n = 4) primary production was 0.04 µmol C $l^{-1}h^{-1}$ (<10 µm) and 0.06 µmol C l^{-1} h^{-1} (>10 µm). Only one "oceanic station" was sampled for primary production. Rates were also low with 0.01 µmol C l^{-1} h^{-1} (<10 µm) and 0.04 µmol C l^{-1} h^{-1} (>10 µm). The rates on time-series station 19 (n = 5) varied between 0.01 - 0.45 µmol C l^{-1} h^{-1} and had mean values of 0.14 µmol C l^{-1} h^{-1} (<10 µm) and 0.29 µmol C l^{-1} h^{-1} (>10 µm). More detailed results will be shown in chapter 4.2.3.

In April 2006 no "coastal stations" were sampled. Production rates in size fractions <10 µm (Fig. 16 A) and >10 µm (Fig. 16 B) were about the same as in April 2007. Total primary production in April 2006 ranged between 0.04 and 0.19 µmol C l^{-1} h^{-1}.

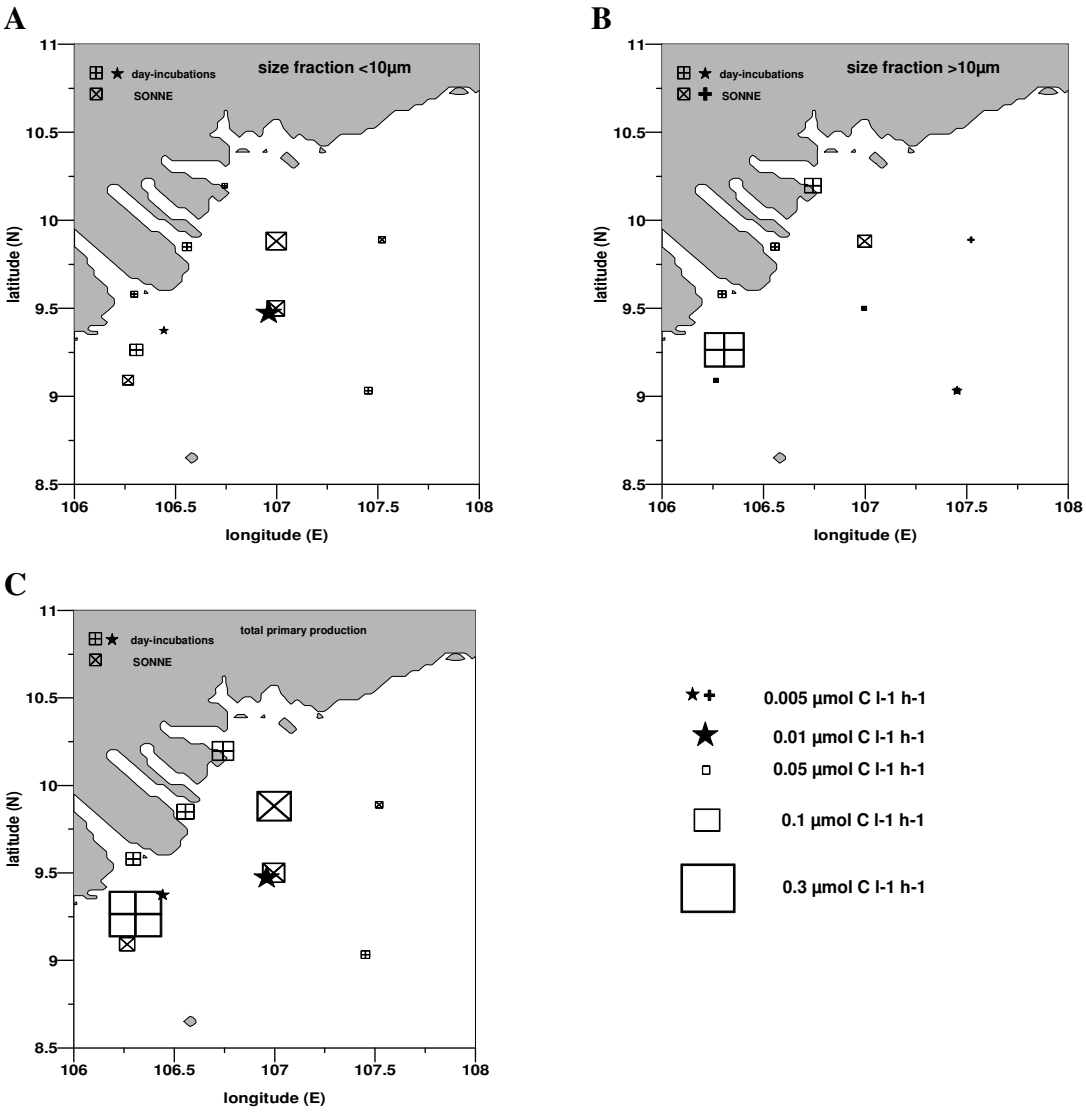

Fig.16: Primary production rates within size fractions <10 µm (A); >10 µm (B) and total rates (C) from April 2006 (SONNE) and April 2007 (day-incubations)

4.1.4 Phytoplankton

4.1.4.1 Cytometry

In the size fraction <10 µm up to eight different picoplankton populations were found. These could be subdivided into four populations of cyanobacteria (C1-C4) and four populations of eukaryotic algae (E1-E4) based on Gasol´s manual (1999) about the FACScalibur flow-cytometer. The cytograms A and B in figure 17 show all detected populations. They were also used to define the populations by plotting orange fluorescence (phycoerythrin) versus red (chlorophyll) and red fluorescence versus side scatter.

A **B**

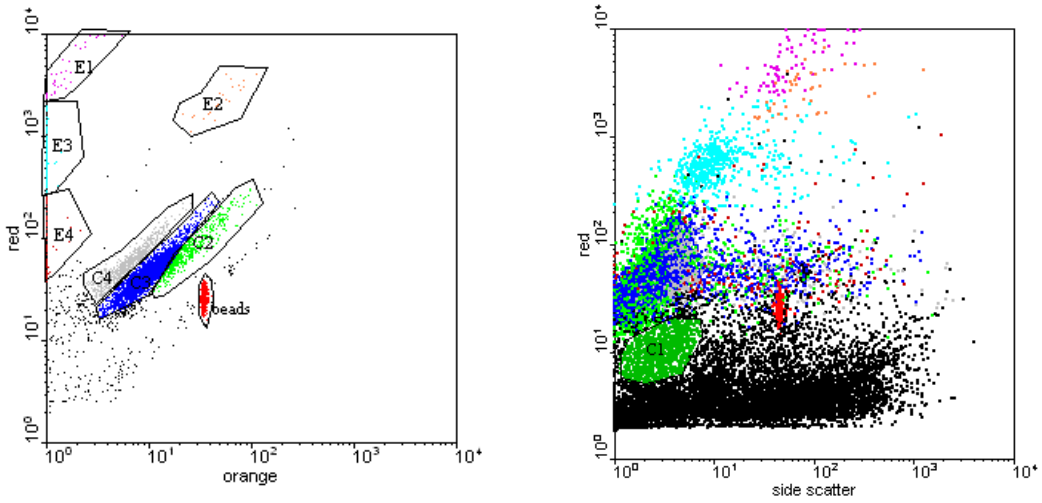

Fig. 17: Cytograms with different picoplankton populations: (A) fluorescence of phycoerythrin (orange) versus fluorescence of chlorophyll (red);(B) side scatter signal versus fluorescence of phycoerythrin (orange)

The cyanobacteria populations C1, C2 and C3 were found at every station. The population C4 was only present at stations nearest to the coast on transects two and three as well as at the time-series station 19. Its density increased from north to south.

The population C1 was identified as *Prochlorococcus* spp. based on its size and the small amount of phycoerythrin. The populations C2, C3 and C4 were located in the red over orange plot were *Synechococcus* spp. is normally found (compare to Marie et al., 1999) and therefore classified as cyanobacteria. However, a more specific taxonomic determination of these populations was not possible.

The eukaryotic algae populations E1, E3 and E4 were found on all stations, the population E2 did not occur on stations classified as “oceanic”. It is not possible to

name the eukaryotic populations taxonomically, but based on the existence of phycoerythrin they could be either Rhodophyceae or Cryptophyceae.

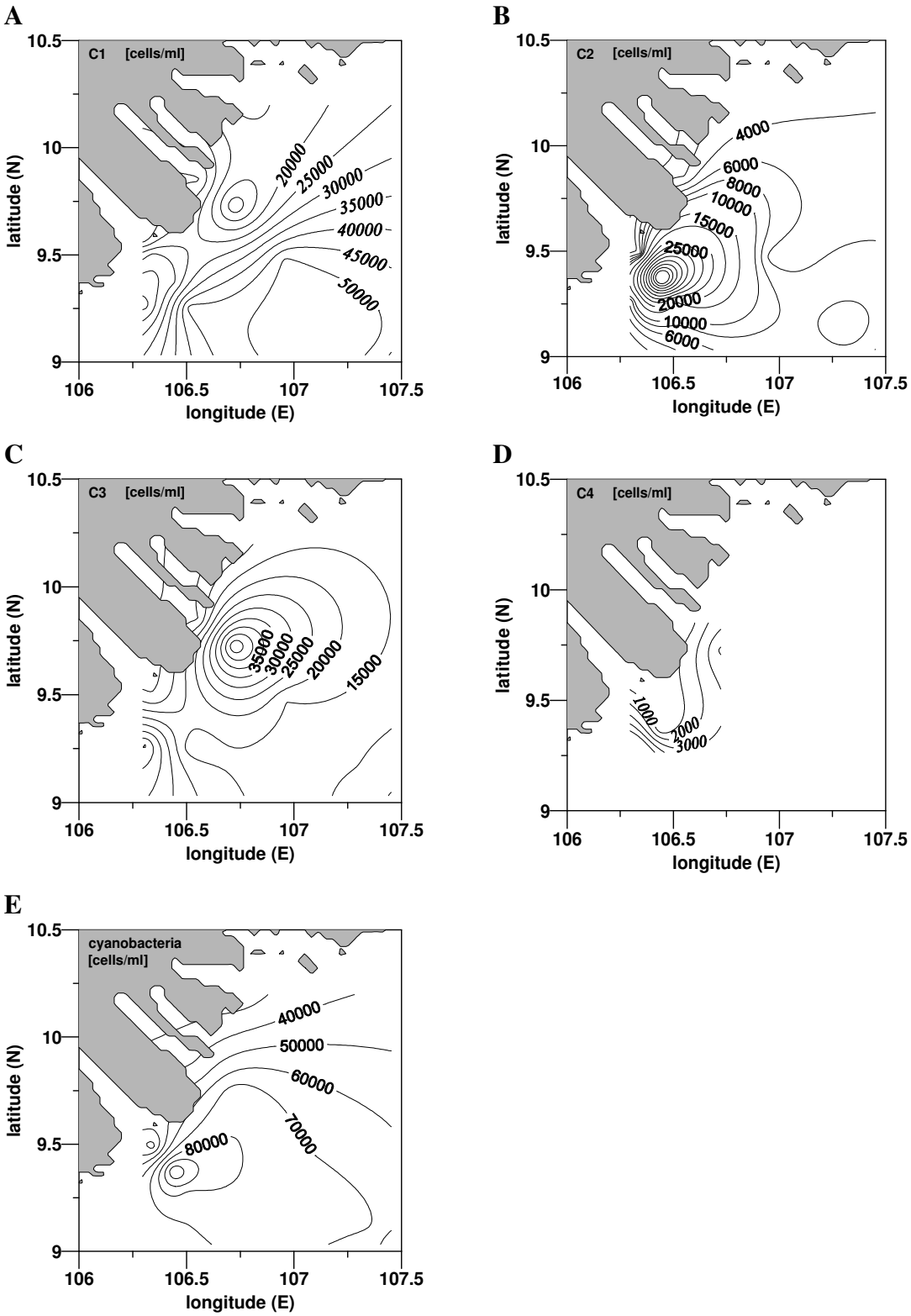

Fig. 18: Horizontal distribution of cyanobacteria populations: (A) *Prochlorococcus* spp. population C1; (B),(C),(D) *Synechococcus* spp.-like populations C2,C3,C4; (E) horizontal distribution of all cyanobacteria

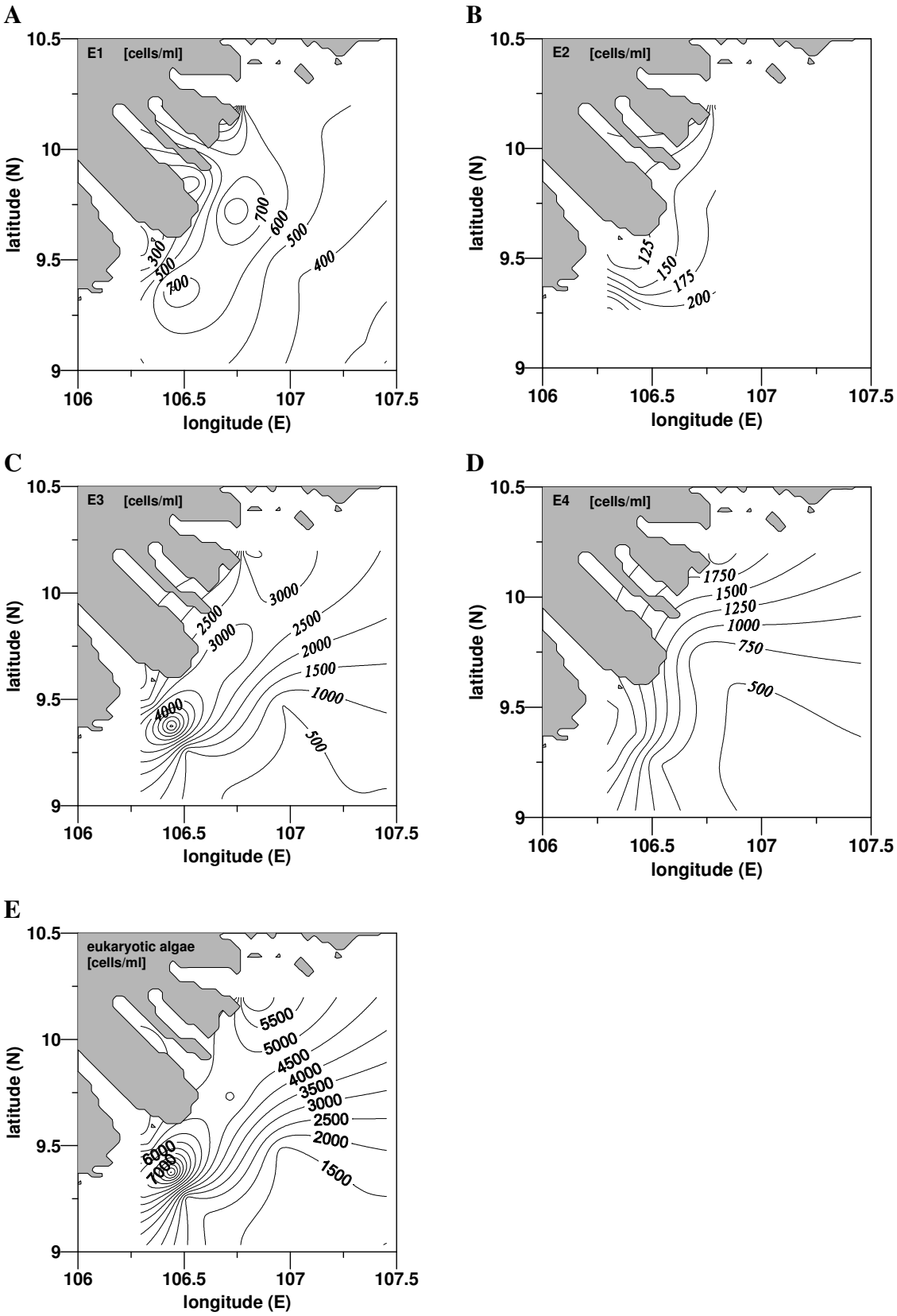

Fig. 19: Horizontal distribution of eukaryotic algae; (A), (B), (C), (D) individual populations E1-E4; (E) total distribution of eukaryotic algae

The cyanobacteria populations contributed ~91% (sd = 6.1%; n = 12) to the overall number of cells. The cyanobacteria population of *Prochloroccocus* spp. (C1) dominated and accounted for ~52% (sd = 26.3%; n = 12) to the total cell number. Density increased towards the open sea and was highest at "oceanic stations" with ~71% (sd = 7.0%; n = 4). Exceptions were made at stations two and three which showed densities >75%. Cell contributions of populations C2-C4 showed high deviations. The populations C2 and C3 reached maxima at "intermediate stations", population C4 increased towards the south. Generally, the overall abundance of cyanobacteria increased with distance to the coast.

Within eukaryotic algae the populations E3 and E4 dominated and contributed ~7% (sd = 5.4%; n = 12) to total cell numbers. These two populations were summarized as picoeukaryots. The populations E1 and E2 were characterized as nanoeukaryots. The cell distribution of E1 showed a plume leading from station 20 (transect 1) towards the south. The cell density of population E2 increased also toward the south. Altogether, the cell abundance of eukaryotic algae decreased from "coastal" to "oceanic stations".

Cell abundance was plotted versus nitrogen fixation rates for each population and total cyanobacteria to identify N_2-fixing organisms.

Tab. 1: Significance for relationship between cell abundance of different populations and nitrogen fixation rates (<10 µm)

population	Nitrogen fixation
C1	n.s.
C2	n.s.
C3	$p \leq 0.1$
C4	$p \leq 0.1$
C1-C4	n.s.

No relationship was found with population C1 which supports the characterization of C1 as *Prochlorococcus* spp. Furthermore, no relationship was found between cell abundance of population C2 and N_2-fixation rates. This could be evidence that population C2 was in fact *Synechococcus* spp. For populations C3 and C4 relationships were found (Tab. 1). This indicates that the actual nitrogen fixing organisms of the <10 µm fraction could be part of these populations, even though not all organisms of each population might perform fixation.

4.1.4.2 Phytoplankton Counts

In the phytoplankton size fraction >10 µm five classes were identified. Chlorophyceae and Dictyochophyceae occurred only at "coastal stations" and showed very low abundances (<1000 cells/l). Hence, they only played a minor role in the phytoplankton assemblage and will not be further discussed. Diatoms (Bacillariophyceae) reached the highest overall abundances (>75.000 cells/l). The distribution was densest in the southwest were the Mekong River had its highest influence (Fig. 20 A). Cyanobacteria (Cyanophyceae) were present on "intermediate" and "oceanic stations" (Fig.20 B) and dinoflagellates (Dinophyceae) occurred at every station (Fig. 20 C).

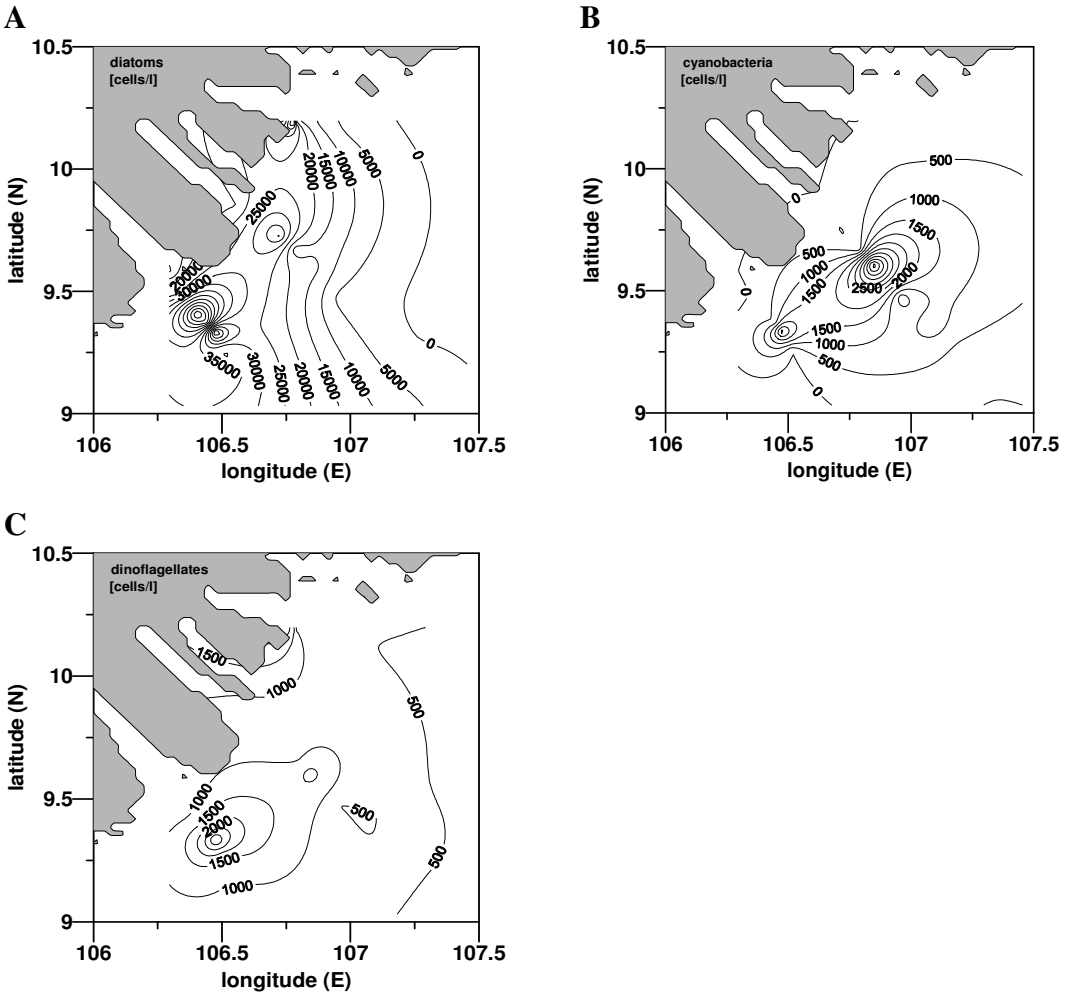

Fig.20: Distribution of major phytoplankton groups: (A) diatoms, (B)cyanobacteria; (C)dinoflagellates

The diatoms included several species of *Rhizosolenia* spp., *Chaetoceros* spp., *Guinardia* spp. and *Hemiaulius* spp., all known as hosts for internal or external diazotrophs. The presence of symbiotic diazotrophs was not proved.

Cyanobacteria included the diazotrophs *Trichodesmium eurythraeum* and *T. thiebautii* as well as the non-diazotroph species *Oscillatoria* sp.

4.1.5 Phycoerythrin

A feature limited to cyanobacteria (and Cryptophyceae and Rhodophyceae) are phycobiliproteins with associated pigments. These pigments form a complex called phycobilisome which is attached to the thylakoid membrane as illustrated in figure 21. The pigments phycoerythrin, phycocyanin and allophycocyanin are able to harvest solar energy at different wavelengths and hence, contribute to photosynthesis (French and Young, 1952).

This work focuses on the phycoerythrins only. The quantification of phycoerythrin can provide information on biomass and taxonomical composition (Lantoine and Neveux, 1997; Neveux et al., 1999), and recent work established the spectral diversity of different species in oligotrophic oceans (Neveux et al., 1999, 2006).

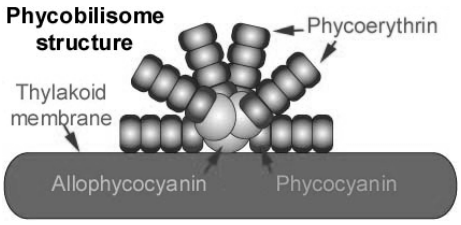

Fig. 21: Structure of a phycobilisome (http://www. botany. hawaii. edu/ faculty/ webb /bot 311 /Rhodophyta/rhodophyta2.htm)

Phycoerythrin samples were taken at 18 stations including seven sampling points at the time-series station 19. Additionally, net-tows were conducted at four of these stations with a 10 µm phytoplankton net.

Total concentration of phycoerythrin could not be determined yet, but measured areas were normalized to the highest value to demonstrate relative differences. Figure 22 shows the distribution of both size fractions.

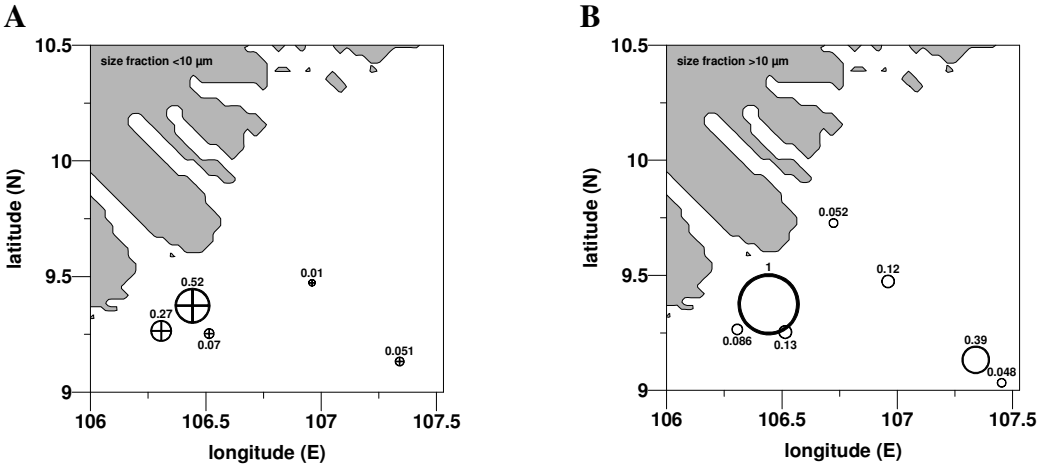

Fig.22: Distribution of phycoerythrin in size fractions <10µm (A) and >10µm (B) from April 2007

No phycoerythrin signals were detected at “coastal stations” because of the high turbidity.

Three “intermediate stations” were sampled including the time-series station with seven sampling points and one net-tow. Station 8 showed the highest measured values in both size fractions. Normalized spectra were illustrated in Fig. 23.

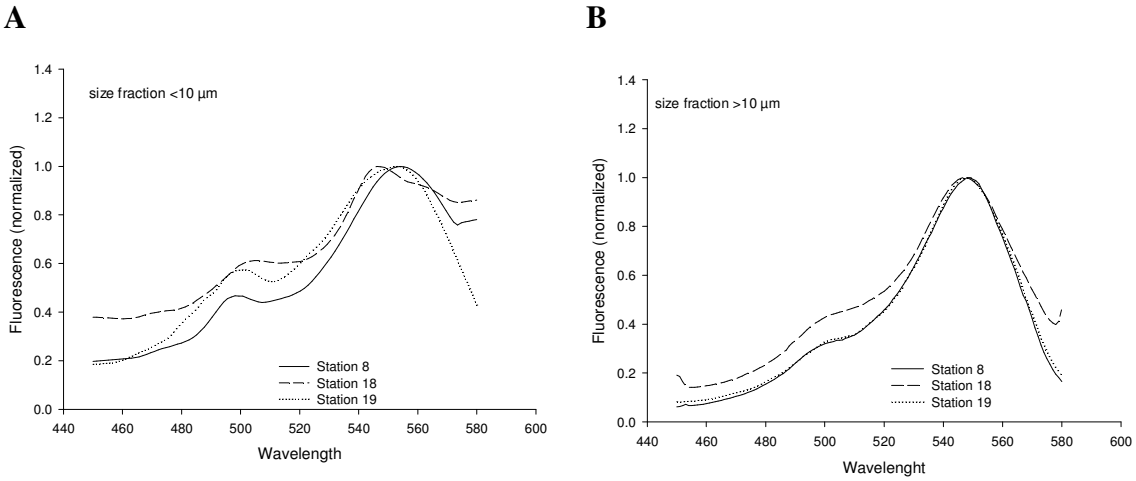

Fig. 23: Fluorescence spectra of intermediate stations: size fractions <10 µm (A) and >10 µm (B), normalized to the PEB-peak

Spectra from the <10µm fraction demonstrated a shoulder at 500 nm and that was associated to PUB which is present at these wavelengths. A second peak associated to PEB was observed at 549 nm ± 3 nm, the resulting PUB/PEB ratio averaged at 0.502 (sd = 0,097; n = 3). In the >10µm size fraction two clear peaks were observed, a PUB-associated one at 499 nm and a PEB-associated peak at 553 nm ± 5 nm. The mean value of the PUB/PEB ratio was 0.502 (sd = 0.159; n = 3). Results from the time-series station will be displayed in chapter 4.2.5.

At “oceanic stations” phycoerythrin was measured in both size fractions. There, the concentration in the >10 µm fraction exceeded the concentrations in the <10 µm fraction, at one station no <10 µm-signal was detected. Net-tows and >10 µm concentrations gave results showing two clear peaks (Fig.24). The PUB-peak had a wavelength of 500 nm ± 2 nm and the PEB-peak appeared at 556 nm ± 2 nm.

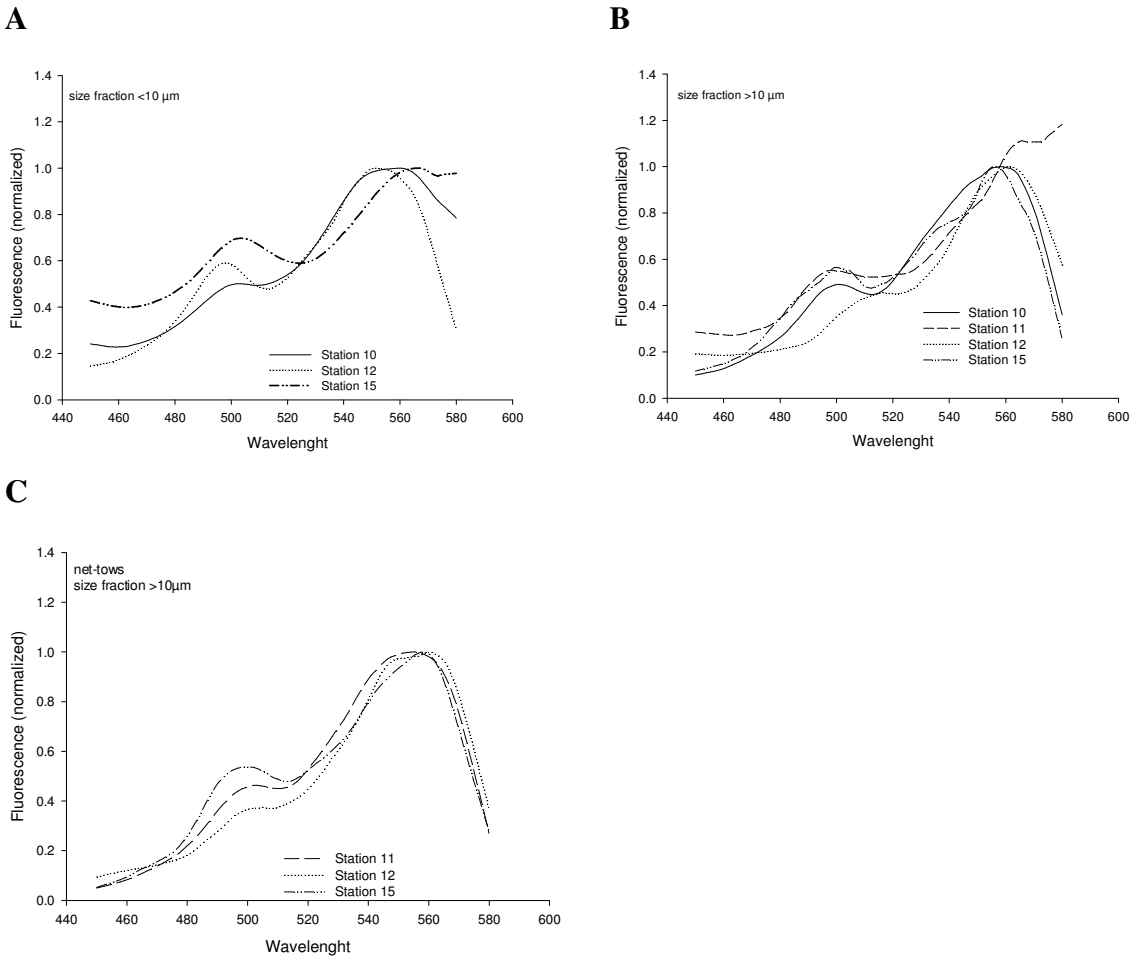

Fig. 24: Fluorescence spectra of oceanic stations; size fractions <10µm (A)and >10µm (B) and net-tows (C), normalized to the PEB-peak

Spectra in both size fractions as well as net-tows exposed two clear peaks. In the <10 µm fraction the first peak was visible at 503 nm ± 2 nm and the second at 560 nm ± 7 nm. The resulting PUB/PEB ratio reached 0.567 (sd = 0.118; n = 3). In the >10 µm size fraction the PUB-associated peak was at 498 nm and the PEB-associated peak at 556 nm ± 2 nm. The mean values of the PUB/PEB ratio was 0.570 (sd = 0.02; n = 3). The net-tow spectra had peaks at 501 nm ± 2 nm and 556 nm ± 2 nm, respectively. The PUB/PEB ratios ranged between 0.380 and 0.537 (mean = 0.463; sd =0.079; n = 3).

Tab. 2: Overview on detected peak-wavelengths and PUB/PEB ratios

Station	size fraction	PUB peak (nm)	PEB peak (nm)	PUB/PEB ratio
1	>	-	-	
1	<	-	-	
2	>	-	-	
2	<	-	-	
3	>	-	-	
3	<	-	-	
5	>	-	-	
5	<	-	-	
8	>	500	549	0,32
8	<	498	554	0,47
10	>	500	557	0,49
10	<	502	552	0,50
11	>	498	558	0,55
11	<	-	-	
11	net-tow	503	555	0,47
12	>	498	554	0,59
12	<	505	562	0,49
12	net-tow	502	554	0,38
15	>	499	555	0,57
15	<	502	564	0,70
15	net-tow	499	558	0,54
18	>	504	546	0,61
18	<	-	-	
19	>	500	552	0,57
19	<	499	557	0,61

4.2 Time-Series Station

4.2.1 Hydrography

The time-series station was sampled seven times overall. Sampling was conducted every three hours during the day and every six hours at night, and started at 05:30 AM on April 18th and lasted until 07:00 AM on April 19th. CTD-casts were executed hourly. Figure 25 illustrates the turn of tides including salinity. Low tide was present at 09:00 AM and 09:00 PM local time on April 18th and high tide was present at 03:00 PM on April 18th and 04:00 AM local time on April 19th.

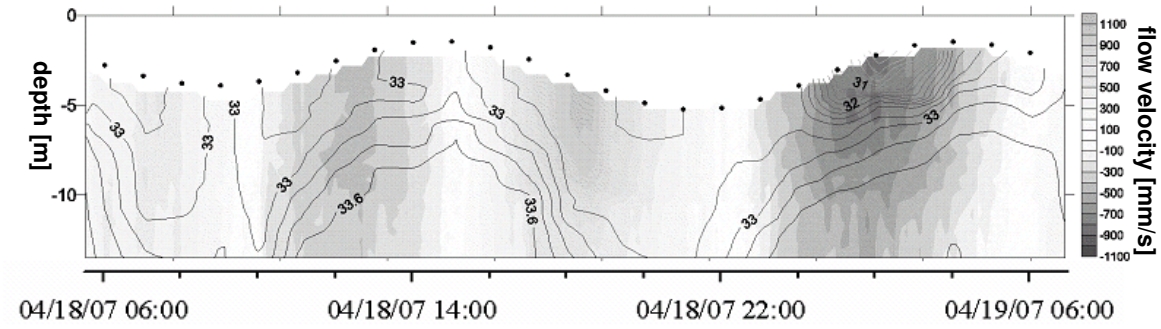

Fig. 25: ADCP profile of time-series station 19 with salinity isolines, tidal cycles, and flow velocity

The temperature profile exposed a range of 1°C over the sampled time with higher values during daylight hours. The salinity ranged within a few PSU with a steep drop between midnight and 04:00 AM (April 19th).

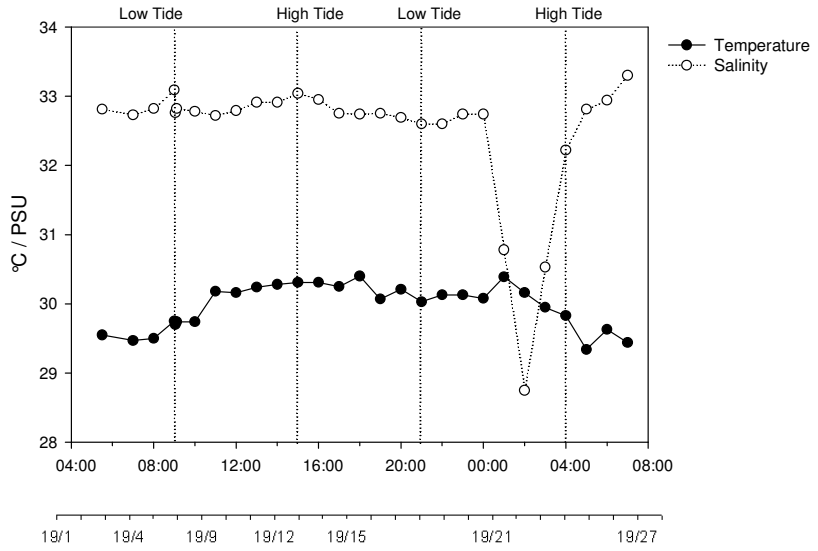

Fig. 26: Temperature and salinity measured hourly at time-series station

4.2.2 Nutrients and Chlorophyll

The nutrient concentrations fluctuated. Within the first observed tidal cycle the higher values coincided with low tide and lower values coincided with high tide. The second tidal cycle lacked sampling the moments of low tide and high tide and therefore can not give information if they concurred with highest and lowest nutrient values, respectively (Fig.27). Low tide-water had the highest content of river water and consequently higher nutrient concentrations compared to high tide-water which had a higher amount of oligotrophic water and nutrient concentrations below detection limits. Overall, nutrient concentrations were low with values comparable to other "intermediate" and "oceanic stations". Based on the relationship of chlorophyll-a- and POC-concentration the station was classified as an "intermediate station" (Fig. 8)

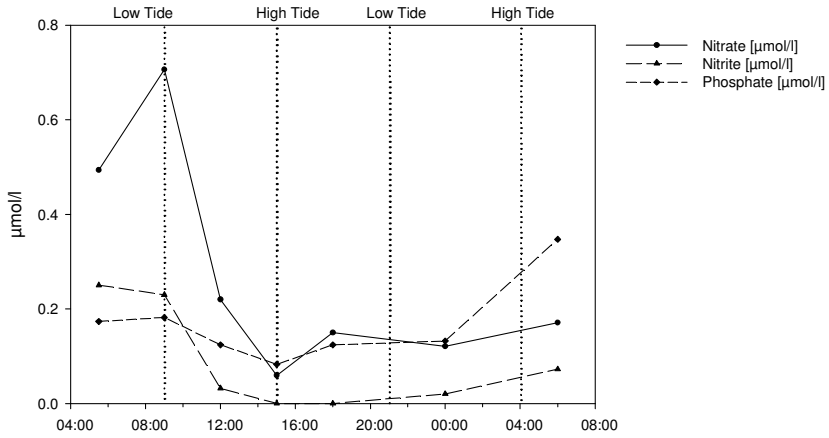

Fig. 27: Course of nutrient concentrations at time-series station

Concentrations of dissolved silicate (Fig. 28 A) demonstrated a similar pattern as the nutrients shown above. Highest values were detected in low tide-water and lowest values coincided with high tide-water. Concentrations were between 4.8 and 10.1 µmol/l and agreed with values measured at other "intermediate stations". The distribution of particulate silicate (Fig.28 B) differed from the nutrients and exposed a second major concentration-maximum in the second tidal cycle. The peak occurred between low and high tide and reached values similar to the first peak (4.0 and 4.1 µmol/l). The lowest concentration was measured in low tide-water with 1.6 µmol/l.

A

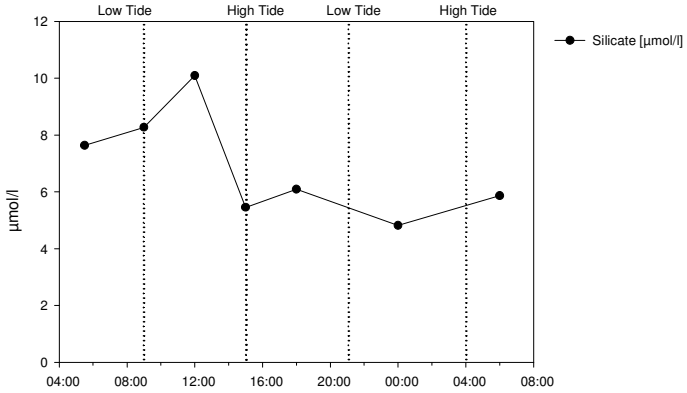

B

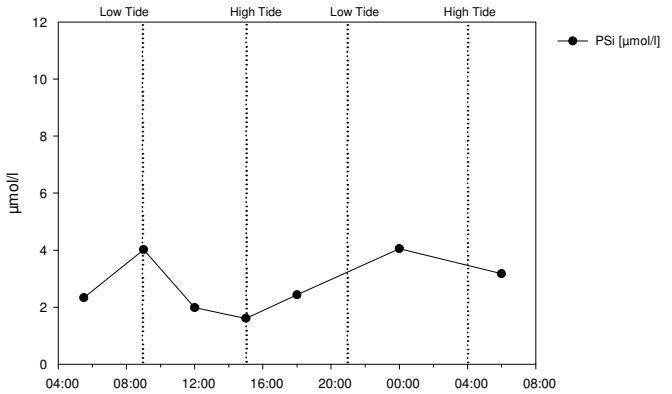

Fig. 28: Course of dissolved silicate (A) and particulate silicate (B) at time-series station

Highest chlorophyll-a concentrations matched with the low tide and stayed at about the same level for all other sampling points (mean = 1.7µg/l; sd = 0.47µg/l; n = 7). At the same time, phaeopigment concentrations remained unchanged (mean = 0.5µg/l; sd = 0.1µg/l; n =7) (Fig. 29). Additionally, the higher chlorophyll-a concentrations at low tide indicate higher abundance of phytoplankton and primary production, which fit to the high concentrations of particulate silicate.

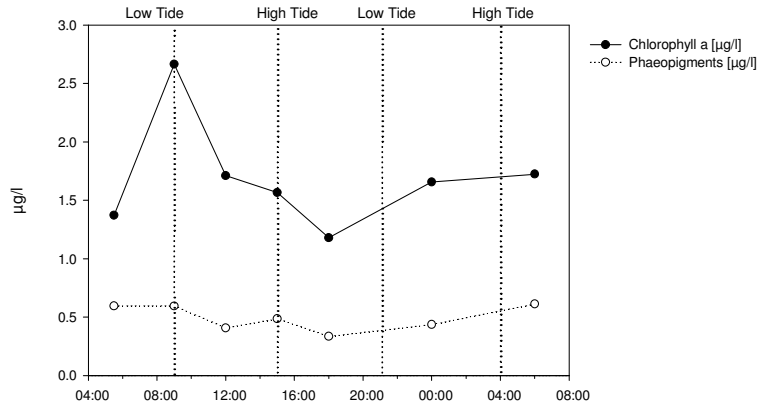

Fig. 29: Course of chlorophyll-a and phaeopigments at time-series station

4.2.3 Nitrogen fixation

Nitrogen fixation rates ranged between 2.63 - 14.36 nmol N $l^{-1}h^{-1}$ in the <10 µm fraction and between 3.38 - 14.47 nmol N $l^{-1}h^{-1}$ in the size-fraction >10 µm. Total N_2-fixation rates were given by the sum of both size fractions.

During the day, N_2-fixation rates for <10 µm size-fraction dominated by magnitudes of ~1.7 to 2.8. At night the >10 µm fraction fixation prevailed fixation by a magnitude between ~1.1 and 3.8. Highest rates were not detected during either high or low tide but in between. This applied for both size-fractions as well as total fixation. Also, no clear pattern of N_2-fixation was seen in the tidal cycles. The discovered pattern of nitrogen fixation rather followed a day-night cycle.

A

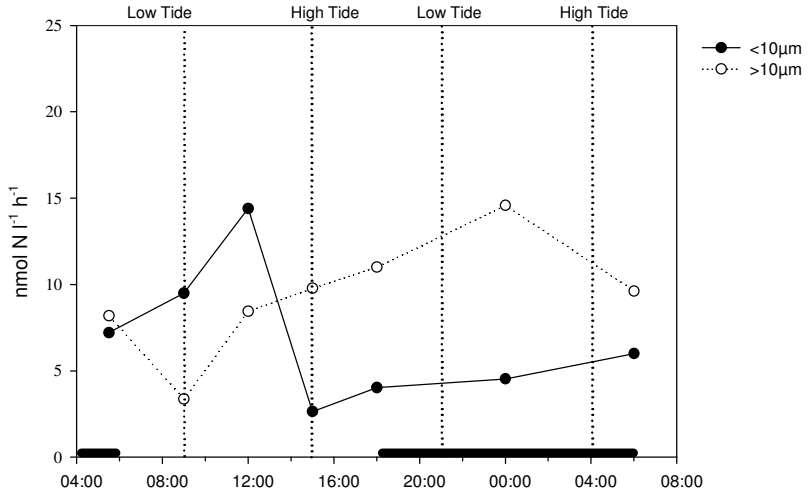

B

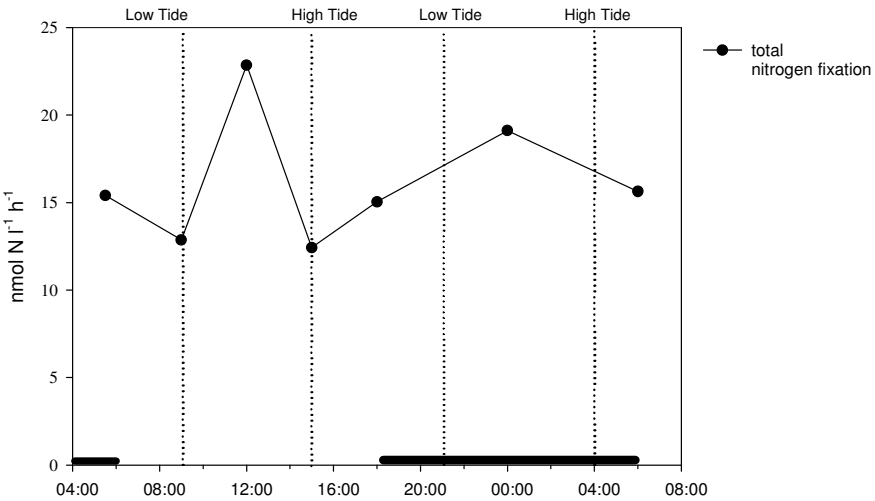

Fig. 30: Course of N_2-fixation in different size fractions (A) and total N_2-fixation (B) at time-series station; black bars indicate night-incubations

Incubations for primary production took place concurrently to nitrogen fixation. No primary production was measured during the night. Primary production rates were dominated by the >10 µm fraction and total production rates were the highest measured during both cruises in April 2006 and April 2007. The production of the >10 µm size-fraction exceeded the production of the <10 µm fraction by a magnitude of 1.6 - 3.0. In April 2006 the dominating size fraction was the <10 µm fraction and dominated primary production by a mean of 2.5 (n = 3).

Around low tide production was higher than during high tide which supports the assumption that oceanic water was less productive than water that carried higher nutrient loads.

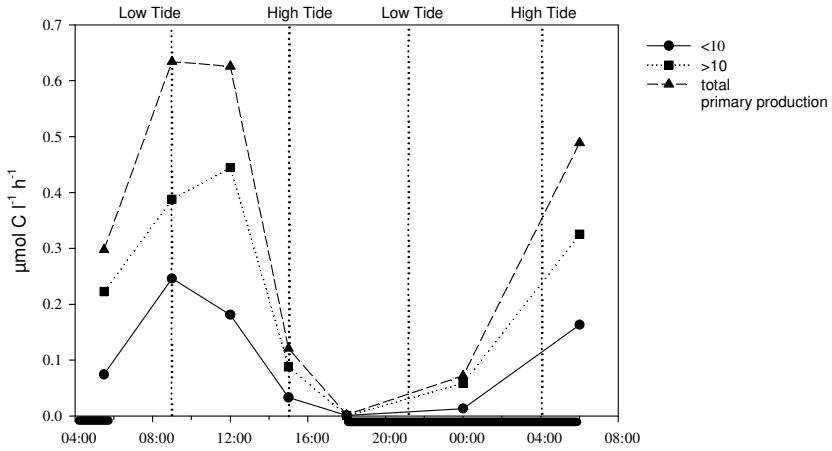

Fig. 31: Course of primary production at time-series station; black bars indicate night-incubations

4.2.4 Phytoplankton

4.2.4.1 Cytometry

The analysis of the samples by flow cytometry established eight different picoplankton populations. These populations were subdivided into four populations of cyanobacteria and four populations of eukaryotic algae (compare to chapter 4.1.4.1). All populations occurred in every sample.

Figure 32 displays the changes within the different populations (cyanobacteria (A); eukaryotic algae (B)) over time. Thereby, the courses of cyanobacteria and eukaryotic algae were opposite. Abundance of cyanobacteria was lower during low tide and increased towards high tide where the maxima in abundances were reached. Unlike the eukaryotic algae which had higher abundances during low tide which decreased towards high tide.

A **B**

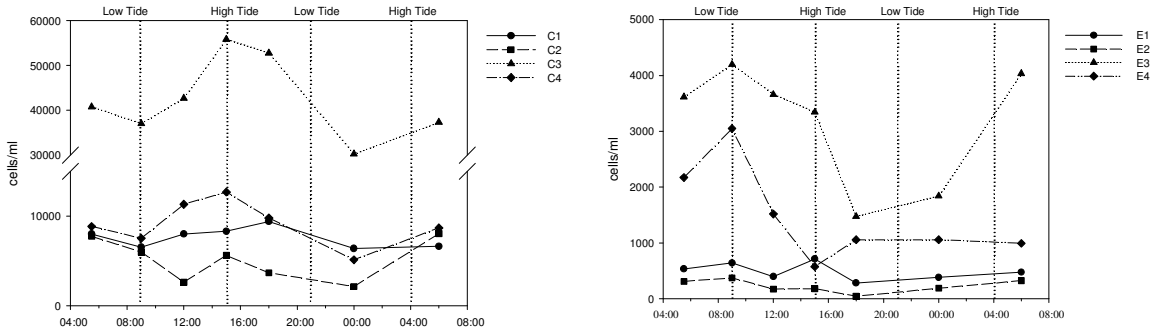

Fig. 32: Course of picoplankton populations: cyanobacteria (A) and eukaryotic algae (B) at time-series station

The time-series station exposed low cell numbers in the C1 and C2 populations compared to all other stations. Opposite to this, the station had high cell numbers of population C3 and the highest abundances of C4 of all stations. The total abundance of cyanobacteria ranged among “intermediate” and “oceanic stations”.

Compared to other stations the dominating population was C3 with ~60.3% (sd = 4.1%; n = 7) followed by population C4 with 12.9% (sd = 1.67%; n= 7). All cyanobacteria together contributed ~91.3% (sd = 2.8%; n = 7) to the total cell number which is identical to the stations sampled on the transects.

The populations E3 and E4 dominated within eukaryotic algae and contributed ~4.6% and ~2.2% to total cell numbers which was the same dimension as on transect stations.

Compared to the stations sampled on the transects the abundance of *Prochlorococcus*-cells per milliliter was among the lowest measured.

The rates of nitrogen fixation in the <10µm fraction and total cyanobacteria abundance are shown in figure 33. Both curves had different courses and indicated no relationship among them.

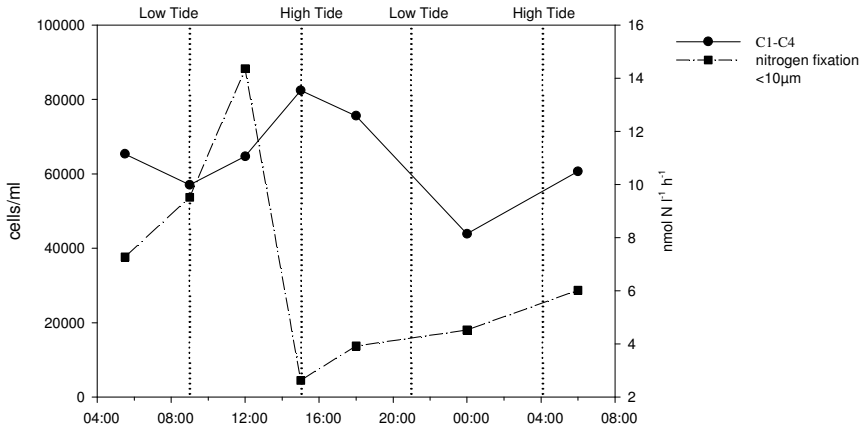

Fig. 33: Course of cyanobacteria abundance and nitrogen fixation (<10 µm) at time-series station

4.2.4.2 Phytoplankton Counts

In the >10 µm size fraction only three classes of phytoplankton were found. The classes Chlorophyceae and Dictyochophyceae were not observed. Diatoms were found at all sampling points of station 19 and dominated with abundance between 38.000 to 262.000 individuals per liter. The highest abundances were found between tides. Within the assemblage a variety of species that are known to act as hosts in diatom-cyanobacterial symbioses, including *Rhizosolenia* spp., *Hemiaulus* spp, *Chaetoceros* spp. and *Guinardia* spp. were observed, but no relationship between diatom abundance and N_2-fiaxtion (>10 µm) was found.

A second class that was detected at all sampling points were dinoflagellates. They reached abundance of 680 to 61.000 cells per liter. Dinoflagellates also had highest abundances between tides. Cyanobacteria were also found but only at two sampling points, one at high tide and one sampled shortly after high tide. The two species *Trichodesmium eurythraeum* and *T.thiebautii* occurred and both showed low abundances of 300 and 150 individuals per liter, respectively.

4.2.5 Phycoerythrin

Phycoerythrin samples at the time-series station included seven sampling points for the size-fractions and one net-tow (>10 µm).

The concentrations from the <10 µm fraction surpassed the >10 µm-concentrations at all sampling points. During the first tidal cycle a constant increase in concentration for the <10 µm fraction was visible, but was not observed in the second tidal cycle (Fig.34 A).

A

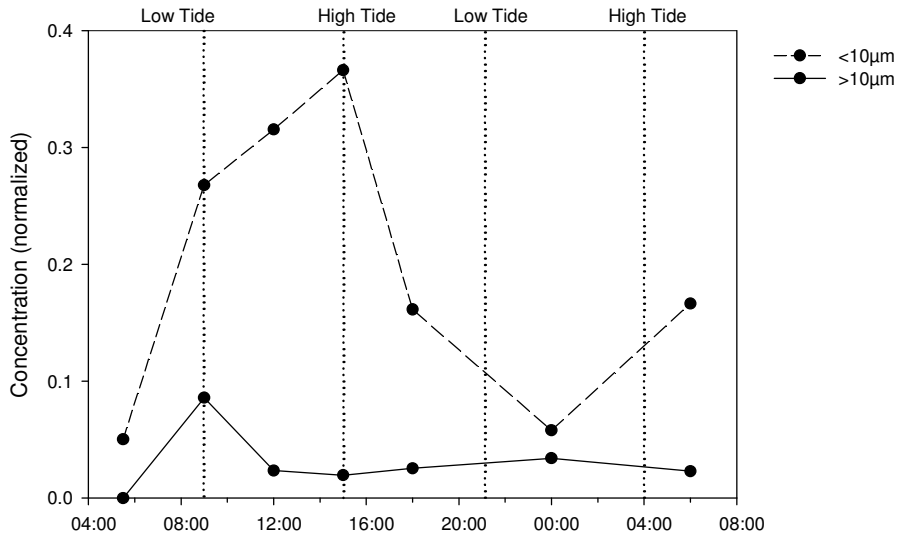

B

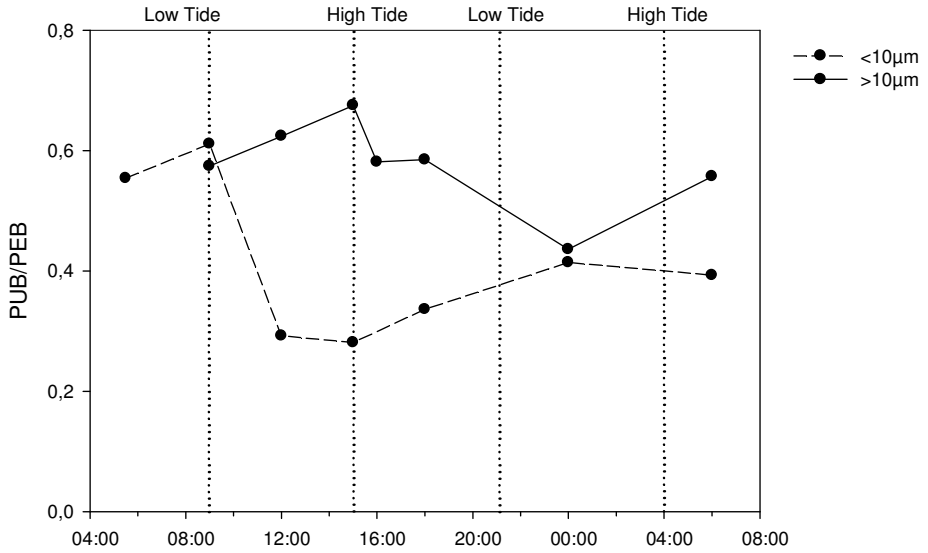

Fig. 34: Course of phycoerythrin concentration (normalized) (A) and PUB/PEB ratios (B) at time-series station

The PUB/PEB ratio was calculated and illustrated in Fig.34 B. The ratios had mean-values of 0.576 (sd = 0.073; n = 7) for the <10 µm size fraction and 0.412 (sd = 0.126; n = 7) for >10 µm.

PUB/PEB ratios of the <10 µm fraction demonstrate higher values during high tide. Opposite to this ratios in the >10 µm fraction showed higher values during low tide. Spectra of the <10 µm size fraction (Fig.35 A) had only one clear peak at 550 nm ± 4 nm. A second peak was not obvious but a shoulder occurred at wavelengths were phycourobilin is present. Therefore, the PUB-fluorescence for calculations was taken at 500 nm. The size fraction >10 µm displayed two clear peaks. At five sampling points the PUB-associated peak occurred at 503 nm ± 2 nm and a PEB-associated peak was present at 560 nm ± 2 nm. Two sampling points, including the net-tow, established a PUB-associated peak at 502 nm ± 2 nm and a PEB-associated peak at 551 nm ± 2 nm.

A

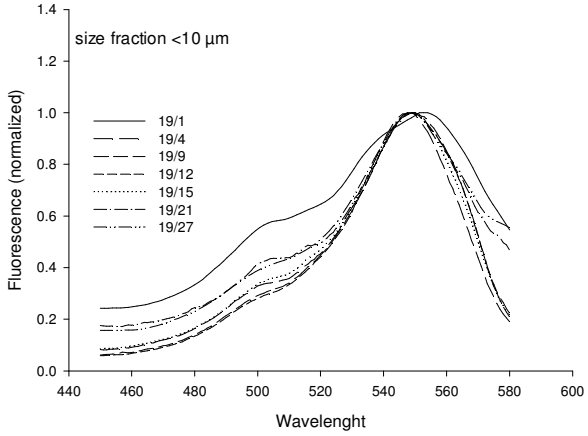

B

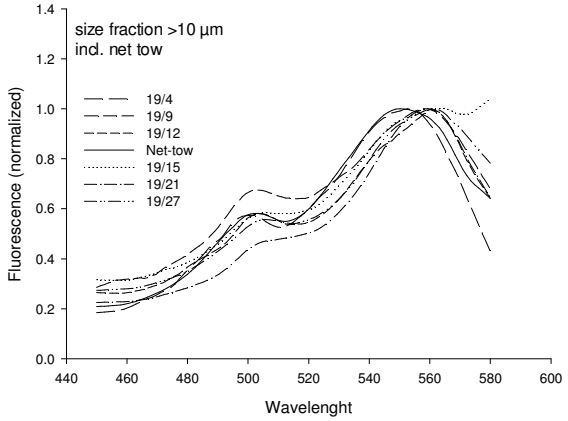

Fig. 35: Normalized fluorescence spectra for all sampling points in size fractions <10 µm (A) and >10 µm (B) at time-series station

Tab. 3: Overview on detected wavelengths and PUB/PEB ratios

Station	size fraction	PUB peak (nm)	PEB peak (nm)	PUB/PEB ratio
19/1	>	-	-	
19/1	<	500	553	0,55
19/4	>	500	552	0,57
19/4	<	499	557	0,61
19/9	>	502	558	0,67
19/9	<	500	549	0,29
19/12	>	504	560	0,58
19/12	<	500	549	0,28
19/13	net-tow	503	549	0,62
19/15	>	504	563	0,59
19/15	<	500	547	0,34
19/21	>	500	560	0,44
19/21	<	500	549	0,41
19/27	>	505	560	0,56
19/27	<	500	547	0,39

5 Discussion

5.1 Critical discussion of methods

A critical reflection of the method is necessary to estimate the reliability of the results. The calculation of N_2-fixation rates is based on the enrichment of particulate organic matter with ^{15}N-tracer. For this purpose, the $\delta^{15}N$-values of PON as well as concentrations before and after the experiment are important. Furthermore, the length of the incubation is needed for the calculation. The different parameters contribute with certain shares to the overall error and are described in detail by Montoya et al. (1996). The incubation time was calculated using the moments of tracer addition and removal from the incubation tubs. Thereafter, the incubation bottles were covered with a black sheet to limit N_2-fixation, but at stations with high loads of suspended matter the filtration was time consuming and could continue for an hour. It is assumed that N_2-fixation was still ongoing to a certain degree until the filters were stored in the freezer, but no estimation on the amount of N_2-fixation can be made. Recalculations of nitrogen fixation rates by changing the incubation time for 30 minutes gave a variation of ± 10%.

Other potential sources of errors are summarized in the following paragraph. Cells from *Trichodesmium* contain gas-vacuoles to assure buoyancy at the surface and are mainly found in the upper 0.5 m of the water column (Capone et al., 1998). Water used for incubations was sampled within the first two meters of the water column and might not have contained the highest possible *Trichodesmium* concentration. Additionally, *Trichodesmium* cells move to the upper part of a Niskin bottle with velocities ranging between 0.1 – 3 mm/s (Walsby, 1991) because of their gas-vacuoles. The incubation bottles were filled trough a hose at the bottom of the Niskin bottle, concluding that *Trichodesmium* cells might have been left in the Niskin bottle or were distributed at different concentrations among the parallels. This would result in underestimated rates. A second important issue is the possible temperature changes during the incubation. The cooling water was exchanged manually with surface water and solar irradiation might have increased temperatures within the incubation bottles at differently over the day depending on the starting time of the incubation. The temperature optimum for *Trichodesmium* ranges between 24 – 30°C for cultures (Breitbarth, 2004) and growing rates decrease for about 30% at temperatures of 32°C. On the other hand, slightly

increased temperatures could enhance biochemical processes like nitrogenase activity (Staal et al. 2003).
Furthermore, the rates among parallels showed high deviations. This might have been caused by the buoyancy of certain algae and resulted in different plankton concentrations within the incubation bottles. High deviations were also observed in the PON and POC values but samples with high N_2-fixation rates also featured high PON and POC values and vice versa.
Currently, no better method to determine N_2-fixation is available. Hence, the detected rates are reliable and can be used in comparison with previously published rates.

Cytometry is a useful tool to distinguish between different plankton populations and the obtained cell numbers are more precise than numbers obtained through epifluorescence microscopy.
The processes of formaldehyde fixation and quick freezing destroy a certain amount of cells in the samples. Those cells can not be recognized in the cytogram anymore and decrease the actual cell number. Lepesteur et al. (1993) specify the variations in cell concentrations using different procedures in chemical preservation and freezing. For the procedure used in this study, chemical fixation with formaldehyde and rapid freezing indicated a variation in cell abundance of ~33%. It is assumed that the proportion of destroyed cells per population among stations stayed within a certain range. Hence, a general change in cell abundance is preferred to absolute cell numbers per millilitre, even though the gained abundances should indicate the same general magnitude.
Furthermore, high loads of detritus or cell fragments can interact with intact cells and result in overestimated abundances.
An additional error can occur through the setting of regions. The areas around the populations are determined subjectively and might not include all cells of one population, but additional cells that are disguised within a gated region.
All in all, the chosen sampling protocol was the best available for this specific sampling cruise and the results gave a plausible picture of the changes within the populations.

As mentioned before, the method for quantifying phycoerythrin is not commonly used. Previously, phycobiliroteins were only estimated by measurements at single wavelengths (e.g. Moreth and Yentsch, 1970; Wyman, 1992). Moreover, they do not account the spectral diversity of phycoerythrins and lead to over- and/ or

underestimation if distinct types (Wyman, 1992). The integration of the area below the excitation spectra partly allows to overcome this problem (Lantoine and Neveux, 1999).

The extant of phycoerythrin signals from Rhodophyceae and Cryptophyceae in marine phytoplankton is not well studied either. Both are common in estuarine and coastal waters (Exton et al, 1983; Billard and Fresnel, 1986). Cryptophyceae are also known to form spatial and temporal blooms (Jaques, 1968; Gieskes and Kraay, 1983). Hence, they might be present in the Mekong area even though no cells were detected during cell counts (>10 µm).

Another error of underestimating phycoerythrin concentrations could be in the extraction process itself. During sonication the samples have to be kept cool because temperature can potentially increase and destroy the analyte molecules (Vaskari and Coyler, 2003). On the other hand, sonication has to persist long enough to disrupt all cells (Furuki et al., 2003) which makes it difficult to elaborate the time for sonication. During sample treatment the solution temperature did not increase but a warming of the sonication probe was noticed.

Furthermore, the amount of phycoerythrin has to be high enough to be detected by the fluorometer. This threshold was sometimes difficult to achieve for both size fraction.

5.2 Stimulation of N_2-fixation during the intermonsoon

The composition of phytoplankton communities depends on varies factors. In river discharge areas conditions like salinity and nutrient-availability show strong gradients and induce quick changes in phytoplankton assemblages. During the investigation period the Mekong River discharge reached its annual minimum (2.100 m^3/s) with medium salinities between 14-30 PSU near the coast. This salinity might be more favorable for marine phytoplankton compared to the highest discharge in September/October when the salinity in river arms can decrease to 0 PSU. Additionally, the observed water temperatures were about four degrees higher than previously reported (Pohlmann, pers. comm.).

The nutrient concentrations decreased rapidly towards the open sea and reached values of 1 µmol/l (NO_3), 0.2 µmol/l (PO_4), and 10µmol/l (Si) when salinity exceeded 30 PSU at “intermediate stations”. Hence, the Redfield ratio fell below 16 and the lack of NO_3

Tab. 4: Ranges of N-fixation in different oceans distributed by different organisms (size fractions)

Location	Depth	N-fixation (nmol N l^{-1} h^{-1})	Size fraction	N2-fixation contribution (%) primary production	Reference
Mekong 2007 (coastal station)	Surface	0.11 - 2.86	total	6 - 15	This study
Mekong 2007 (intermediate station)	Surface	6.17 - 22.86	total	13 – 163	This study
Amazon River plume (bloom station)	Surface	0.46 - 18.52	*Hemiaulus/Richelia*	25	Carpenter et al. (1999)
Eastern tropical Pacific	pigment max. (10m)	Up to 1.85	*Rizosolenia/Hemiaulus*		Montoya et al. (2004)
Mekong 2007 (ocean station)	Surface	3.96 - 16.10	total	152	This study
Mekong 2006	Surface	0.066 - 0.26	total	0.2 - 2	This study
Arabian Sea	0 - 0.5 m	~10.75	*Trichodesmium*	13	Capone et al. (1998)
Gulf of Mexico	Surface	0.011 - 0.23	*Trichodesmium*		Mulholland et al. (2006)
New Caledonia	Surface	0.23 - 0.85	*Trichodesmium*		Mulholland et al. (2006)
Station ALOHA & Kaneohe Bay	Surface /25 m	0.01 - 0.15	small diazotrophes		Montoya et al. (2004)
Arafura Sea	50-60 m	20 - 62	small diazotrophes		Montoya et al. (2004)
Eastern tropical Atlantic	50 m	2.2	small diazotrophes/ heterotrophic	1 - 12	Voss et al. (2004)
Kaneohe Bay	Surface	0.053	<10µm		Zehr et al. (2007)

became an advantage to nitrogen fixing plankton. At the same time, Si-concentrations were still favorable for diatom growth (Carpenter et al., 1999; Voss et al., 2006).

The N_2-fixation rates measured at "intermediate stations" can be compared to rates determined by Carpenter et al. (1999) in the Amazon River plume (Tab. 4). At several stations the overall fixation rates of the Mekong plume even surpassed the rates found in the Amazon River plume. The Amazon River investigation took place during the lowest annual discharge and also sampled the Orinoco River plume that enters the Atlantic Ocean further north. The dominant diatom/cyanobacterial association in this plume consisted of *Hemiaulus hauckii* and *Richelia intracellularis*, and the bloom extended over a distance of 2.500 km. The observed Mekong River plume was much smaller due to lower freshwater discharge (approx. 15 times less) and nutrients were still above detection limit within the Mekong plume. However, the salinity range (31.5-33.5 PSU) was similar. On the other hand, the species diversity of diatoms was higher in the Mekong estuary and might be an advantage for different symbionts.

Tab. 5: Overview on N_2-fixation in the different size fraction

	N_2-fixation (nmol N l^{-1} h^{-1})	
	range	mean ± sd (n)
"Coastal stations"		
>10 µm	0.03 - 1.29	0.40 ± 0.51 (5)
<10 µm	0.08 - 1.57	0.73 ± 0.55 (5)
"Intermediate stations"		
>10 µm	1.90 - 14.58	8.36 ± 4.07 (8)
<10 µm	2.64 - 14.41	6.57 ± 3.82 (8)
"Oceanic stations"		
>10 µm	0.54 - 15.03	5.52 ± 8.24 (3)
<10 µm	1.07 - 10.81	4.95 ± 5.16 (3)

Voss et al. (2006) postulated that waters with salinities >33.5 PSU do not have increased nitrogen fixation and are therefore not influenced by river water anymore. Two "oceanic stations" with salinities >33.5 PSU exhibited N_2-fixation, so the salinity can not be considered as an indicator for possible N_2-fixation, at least in the investigation in April 2007. Additionally, a high density of visually observed *Trichodesmium* spp. tufts at stations with salinities between 33.0 and 34.0 PSU support

the assumption that blooms are possible in these waters. The distribution of N_2-fixation between both size fraction reverses among two sampled stations (11 and 15). At station 15 high rates were detected in the >10µm fraction which reflect values detected in a *Trichodesmium* bloom in the Arabian Sea (Capone et al., 1998). Furthermore, a δ^{15}N-PON value of 1.5‰ indicated the presence of N_2-fixation in the >10µm size fraction sampled when sampled with a 10µm net. Station 11 showed low levels of N_2-fixation in the >10µm fraction and colonies of *Trichodesmium* were also not observed. However, a δ^{15}N-PON value of 3.9‰ from a net tow was much lower than δ^{15}N-PON value from the GF/F, where a δ^{15}N-PON of 9‰ indicated no presence of N_2-fixation. Thus, N_2-fixation was accomplished in the >10µm size fraction at some point.

In April 2006, only low rates of N_2-fixation were detected at stations close to stations sampled in April 2007. There are no obvious reasons for the differences, δ^{15}N-PON values of 3.5 and 3.6‰ (compared to ≥ 6.0‰ at other stations) from 2006 also suggest that fixation occurred. This may indicate a stable plankton community that is fixing nitrogen for some time already or a degrading plankton community that was fixing nitrogen.

The high fixation rates may also lead to the conclusion that iron did not act as a limiting factor in the investigation cruise in 2007. The river itself probably carries high loads of trace metals (Nittrouer et al., 1995) and atmospheric deposition might have added extra iron (Wu et al., 2003). In oligotrophic seas P and Fe co-limitation can occur and diazotrophic production can be stimulated by dust addition (Mills et al., 2004). *Trichodesmium* even seems to have adapted to the dust input by assimilating iron dust directly (Rueter, 1988) as well as release cell lysate that is able dissolve iron dust (LaRoche and Breitbarth, 2005).

By comparing the rates of primary production and chlorophyll-a between the cruises in 2006 and 2007 significant differences were visible. On the other hand, the ratio between fixed carbon (µmol C) and chlorophyll-a (µg) was similar. The nitrogen fixation rates did not have similar ratios which could lead to the conclusion that either both processes are not directly linked or that the plankton assemblage was different in both years.

Tab. 6: Primary Production and Chlorophyll-a detected in Mekong plume

	"Intermediate stations"		"Oceanic stations"	
	Primary Prod. µmol C l^{-1} h^{-1}	Chlorophyll-a µg l^{-1}	Primary Prod. µmol C l^{-1} h^{-1}	Chlorophyll-a µg l^{-1}
April 2006	0.09 ± 0.03 (3)	0.28 ± 0.08 (3)	0.04 (1)	0.145 (1)
April 2007	0.52 ± 0.16 (5)	1.82 ± 0.48 (10)	0.05 (1)	0.32 ± 0.09 (4)

In order to evaluate the importance of nitrogen fixation in the Mekong River plume the contribution of N_2-fixation upon primary production can be calculated. This was achieved by calculating the proportion of N_2-fixation on the amount of nitrogen necessary to achieve the measured primary production. Therefore, a theoretical C:N ratio of biomass (6.6) was used .

During earlier cruises in the upwelling region of the SCS N_2-fixation and primary production were also determined. It was shown that N_2-fixation rates were 10-fold higher during south-west monsoon than during intermonsoon. Voss et al. (2006) inferred that this was achieved by the influence of the river plume which affected this area. At that time between 0.2 - 2.9% (intermonsoon) and 0.1 - 8.2% (south-west monsoon) of the N-demand were satisfied by N_2-fixation (Voss et al., 2006). In April 2006 this had an overall range between 0.2 - 1.3 % for all investigated stations and showed only slight differences within each size fraction even though the contribution of the >10 µm fraction always exceeded the <10 µm fraction. Consequently, these inputs agree with previous ones from the intermonsoon.

The demand of nitrogen satisfied by N_2-fixation in 2007 showed a completely different picture. The proportion of N_2-fixation on N-demand revealed values that were closer to the ones found in other areas with high nitrogen fixation (Capone et al., 1998; 2005; Carpenter et al., 1999). At "coastal stations" this contribution ranged between 6.8 - 15.4% (n = 3) with a 3 to 4 -fold higher contribution of the <10µm fraction. Regarding the "intermediate stations", the inputs accounted for 23.24% ± 8.9% (mean ± sd;) for 4 sampling points and no clear domination of one size fraction was visible. A fifth station (station 19/sampling point 4) marked an exception. Here, N_2-fixation met 163% of the N demand and fixed nitrogen could even be exported. Both size fractions fixed more nitrogen then needed for primary production within their size fraction. For the only considered "oceanic station" the same picture emerged; nitrogen fixation exceeded

demands by 53%. The extra nitrogen is provided only by the <10 µm, whereas >10 µm satisfied ~8% of the overall demand at this station.

5.3 Symbiotic and unicellular diazotrophs are primary N_2-fixers

At "coastal stations" the provided nutrient concentrations were high and N:P ratios >16 initiated biomass buildup near the coast (Voss et al., 2006). Surprisingly, nitrogen fixation was also measured at stations closest to the coast when concentrations of combined nitrogen were high enough to favor N-uptake over N_2-fixation. The rates ranged between 0.03 -1.28 nmol N l^{-1} h^{-1}, which are comparable with total rates detected by Voss et al. (2006) in oligotrophic waters of the SCS. A few individuals of diazotroph-host species were found at these stations but it is also possible that the fixation was achieved by microorganisms attached to detritus because nitrogen fixation rates in both size fractions were equal. A genetic analysis of *nifH* might give an answer to the question of who was responsible for this N_2-fixation.

Even though, diatom-associated symbionts were not directly observed they were assumed to be present. This assumption was based on the high abundance of observed diatoms known to host diazotrophs and high observed N_2-fixation rates. The detected rates range among the highest published (Tab. 4). A low cell number of *Trichodesmium* spp. was present at some "intermediate stations" which made it difficult to distinguish between the contributed N_2-fixation of symbionts and *Trichodesmium*. At least the N_2-fixation measured at night (>10 µm) can be accredited to diatom associated diazotrophs since Trichodesmium does not fix nitrogen at night (Capone et al., 1997).

Phytoplankton counts in the size fraction >10µm revealed that host species of *Richelia intracellularis* and *Calothrix rhizosoleniae* were found at "coastal", "intermediate" and "oceanic stations" in different abundances. The genus *Chaetoceros* was the most abundant and present at almost every station. It is known to form symbioses with the epibiont *Calothrix rhizosoleniae* (Carpenter, 2002) and was proofed to establish symbioses with *Richelia intracellularis* in the western Pacific Ocean (Gómez et al., 2005). In this study it reached cell numbers of up to 80.700 individuals per liter. Another genus associated with this symbiont is *Bacteriastrum* which was also found at various stations with maximum cell numbers of 5.400 individuals per liter.

The other symbiont *Richelia intracellularis* has been found in the diatom genera *Rhizosolenia*, *Guinardia* and *Hemiaulus* (Villareal, 1992), all of them detected in samples from the cruise. Among those three, *Rhizosolenia* obtained maximum abundances of 6.300 individuals per liter.

Further offshore the impact of the river weakened and became more favorable for the genus *Trichodesmium*. First, an increase in light penetration, caused by a decreasing amount of detritus, favors growth of *Trichodesmium* (Carpenter 1983, Carpenter et al., 1993). Furthermore, the decrease in dissolved silicate concentration with increasing distance to the coast may had a growth limitation on diatoms and consequently allowed *Trichodesmium* to take over. A decline in diatom abundance was proofed by phytoplankton counts. "Oceanic stations" exhibited combined nitrogen concentrations of $\leq$1 µmol that have no negative effects on N_2-fixation rates even though *Trichodesmium* may additionally take up combined nitrogen (Mulholland et al., 2001; Holl and Montoya, 2005).

The detection of different diazotrophs and estimation of their biomass was attempted by phycoerythrin measurements. The low concentrations in the >10µm fraction mostly resulted in signals difficult to detect, and it was complicated to interpret these spectra. Opposite to that, net tows gave good spectra that made it possible to infer the spectrum to a species. The peak-wavelengths observed at station 15 (499 nm and 558 nm) agree with the PUB/PEB wavelengths for *Trichodesmium thiebautii* published by Neveux et al. (2006). Furthermore, the plankton counts confirm that *Trichodesmium thiebautii* was the only present Cyanophyceae at this station. The net-tows at station 11 and 12 showed slightly different peaks (503/555 nm and 502/554 nm) while no *Trichodesmium* was observed. Nevertheless, the Cyanophyceae *Oscillatoria* sp. was present at both stations and hence could be the dominant species that accounted for the spectra. The discovered peaks do not match any other species known so far.

All PUB/PEB ratios from this study ranged between 0.28 - 0.70. Comparable values (0.4 -0.6) have been found between the coast of western Africa and the Cape Verde Islands and a shifts in the ratio occurred when another water mass was sampled (Lantoine and Neveux, 1999).

Nitrogen fixation in the <10µm fraction was detected at all stations. Unicellular diazotrophic cyanobacteria reach high abundances in tropical and subtropical waters and might therefore contribute equal or even higher shares to global N_2-fixation than the >10 µm fraction (Zehr et al., 2001; Montoya et al., 2004). At stations closest to the coast rates of the <10µm fraction were below 1.6 nmol N l^{-1} h^{-1} and dominated N_2-fixation. These rates were either achieved by unicellular diazotrophic cyanobacteria, by bacterioplankton, or both. Table 5 gives an overview on how much was fixed at the different stations types (<10 µm). Hereby, "coastal stations" showed lowest rates.

"Intermediate stations" showed highest N_2-fixation rates during day and night. The community structure of free living pico- and nanoplankton within a diatom/cyanobacterial association has not been described yet, but flow cytometry data suggested that at least part of the N_2-fixation is achieved by *Synechococcus*-like cyanobacteria. Falcón et al. (2004) proved N_2-fixation by unicellular cyanobacteria only during nighttime (both in the Atlantic and Pacific Ocean), even though, *nifH* transcripts from α- and γ-proteobacteria were present during both night and day.

An additional contributor to this fraction could be *Richelia intracellularis* which was found unattached to any host in the Kurioshio Current south of Japan (Gómez et al., 2005). Unicellular diazotrophs were proven to fix nitrogen at higher NO_3 concentrations in the Atlantic Ocean (Voss et al., 2004) and organisms possibly responsible were identified as Group A cyanobacteria and γ-proteobacteria by Langlois et al. (2005). These rates were measured in depths of about 50 m and the ability of fixing at only 20% light irradiance might be to their advantage in greater depths or in turbid waters such as in the vicinity of the Mekong River.

Nitrogen fixation rates at the "oceanic stations" were variable with rates differing by several orders of magnitude. Additionally, N_2-fixation was measurable during day and night incubations. This suggests a very diverse community structure, which is supported by a high diversity of *nifH*-genes in the South China Sea, including *Trichodesmium*, symbionts, Group A and Group B cyanobacteria as well as α- and γ-proteobacteria (Moisander, pers. comm.).

A negative relationship in abundance between N_2-fixing *Crocospheara* and *Trichodesmium* was described for the south-western Pacific (Campbell et al., 2005) and could explain the different rates measured at stations 12 and 15. While station 15 had high cell numbers of *Trichodesmium* related to high N_2-fixation rates in the >10 µm fraction, no *Trichodesmium* was observed at station 12. Instead, N_2-fixation in the <10

µm fraction was high and might indicate that *Crocosphaera* was able to outcompete larger cells for nutrients like PO_4 (Church et al, 2005). These unicellular diazotrophs can occur in abundance of a few to 1000 cells/ml in the Pacific Ocean (Montoya et al., 2004), but their cell morphologies allows them to disguise in the cytogram among other non-diazotroph *Synechococcus* (Zehr et al., 2007) and microscopic evaluation is necessary to give exact numbers. The spatial and diel variability in N_2-fixation observed in the SCS has also been found in the subtropical North Pacific where it results from a diverse community structure within unicellular cyanobacteria (Zehr et al.2001).

The flow cytometry data of this study suspected the unicellular diazotrophes within the populations C2 and C3. Furthermore, a change within the separate populations was observed along the cruise track. Highest abundance of pico- and nanoeukaryots occurred close to the coast and decreased to <1000 cells/ml at "oceanic stations". The overall abundance of unicellular cyanobacteria increased with growing distance to the coast but the highest abundances were found at "intermediate station" 19. *Prochlorococcus* increased towards "oceanic stations" but exceeded *Synechococcus* spp. (C2) only by one order of magnitude or less and not as described by Campbell et al. (2005) by two orders of magnitude for oligotrophic waters. Consequently, the described "oceanic stations" are no "real" oligotrophic stations. Further genetic analysis are necessary to provide support for the identification of responsible diazotrophs.

Furthermore, the detected phycoerythrin spectra were mixed signals from all those different populations. Estimations of biomass and prediction of possible phytoplankton species as proposed by Neveux et al. (2006) will not be efficient for coastal areas when community structure is as diverse as in the investigated area. Furthermore, it can not be used to forecast probable N_2-fixation (no significant relationship was found). On the other hand, the number of cell abundance of *Synechococcus*-like organisms (populations C2, C3 and C4) correlated very well with the measured concentration of phycoerythrin (<10 µm) (Fig.36).

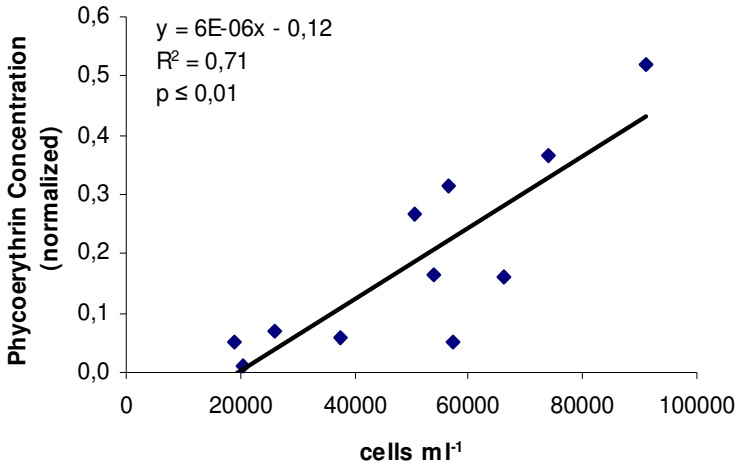

Fig. 36: Relationship between cell number (populations C2-C4) and phycoerythrin concentration (normalized)

The fluorescence spectra were more distinct in the <10 µm fraction, especially at "intermediate stations", but correlation between total chlorophyll-a and total phycoerythrin (normalized) were not significant (Fig.37 A). However, a significant correlation between total chlorophyll-a and phycoerythrin from the <10 µm fraction was detected (Fig.37 B). This leads to the conclusion that picoplankton community dominated the chlorophyll-a biomass.

A

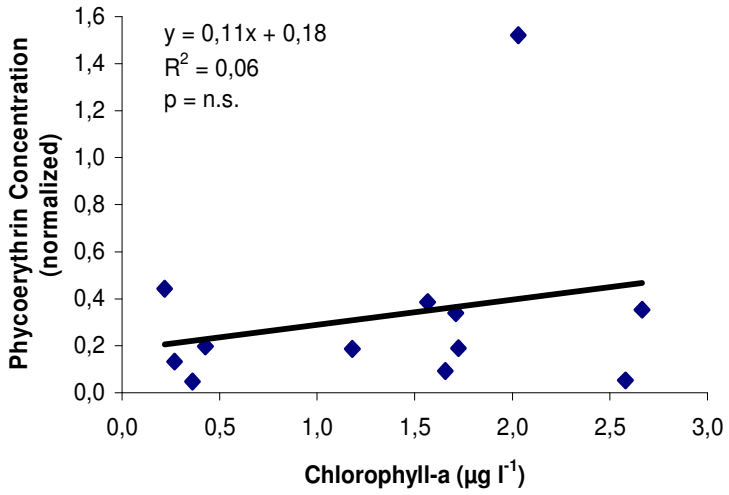

Fig.37: Relationship between total chlorophyll-a and total phycoerythrin (normalized) and chlorophyll-a (A)

B

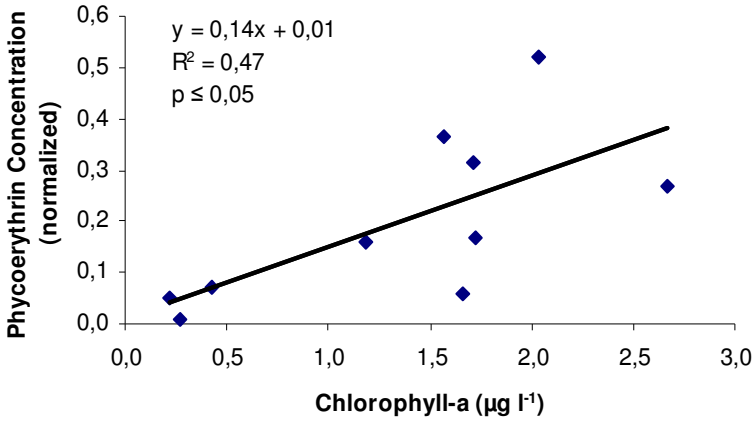

Fig. 37: Relationship between total chlorophyll-a and total phycoerythrin (normalized) and chlorophyll-a (A); and total chlorophyll-a and phycoerythrin of <10µm fraction (normalized) (B)

High-PEB *Synechococcus* seem to play a significant role in coastal, mesotrophic or eutrophic areas (Olsen et al. 1988, 1990) which did coincide with the findings presented. No Synechococcus with high PUB/PEB ratios in <10µm were found, hence, they are supposed to be more widespread in the open ocean and in greater depths (Olsen et al., 1988; Lantoine and Neveux, 1997). The PUB/PEB variety in the <10µm fraction probably reflected the changing proportions of different cyanobacteria-populations as well as different genotypes of *Synechococcus* (Toledo and Palenik, 1997).

The time-series station was supposed to expose changes in N_2-fixation and phytoplankton abundance with the changing tides. The time interval between samplings was very little and gave a good resolution. Also, two complete tide cycle were sampled, one during daytime and one during night. The tide cycles were also visible in the distribution of nutrients, when low tide water contained higher concentrations related to river water and high tide water exhibits lower concentrations of more oligotrophic ocean water.

The courses of silicate and chlorophyll-a did not show this pattern which was probably related to an active phytoplankton community. Other facts that supports the theory of a very active phytoplankton community were the high rates of N_2-fixation and primary production.

Instead of a tidal pattern it is rather assumed that a diel pattern was prevailing. During daylight the dominating size fraction was >10 µm. This changed during the night when the <10µm fraction showed the highest rates. Without further genetic analysis identification of the responsible organisms will be difficult, but it is known that different genotypes of unicellular diazotrophs exist (Zehr et al. 1998; Zehr et al. 2001),

and that their daily pattern of gene expression coincides with the diel cycle of N_2-fixation (Colón-López et al., 1997). Zehr et al. (2007) as well as Church et al. (2005) described so-called Group B unicellular phylotypes fixing nitrogen at night whereas heterocystous and so-called Group A unicellular cyanobacterial phylotypes fix nitrogen during the day. Both groups (A and B) might differ in size whereas Group A cyanobacteria could be smaller and hence, indistinguishable to *Synechococcus* in flow-cytometry. This makes it difficult to confirm their presence and achieve fast enumeration as performed by flow cytometry. It is also possible that they lack phycoerythrin and thus be difficult to identify as cyanobacteria in a cytogram (Zehr et al., 2007).

Instead of a clear change of primary production within a tidal cycle a daily course was observed with increasing rates until midday/early afternoon.

The changes of phycoerythrin concentrations were difficult to interpret. Even though, it is obvious that phycoerythrin prevails in the <10 µm fraction no other provable conclusions can be drawn from the changes in concentration.

Both size fractions showed constantly changing PUB/PEB ratios. Therefore, it is unclear whether the changes were related to a different community structure within the plankton community (Toledo and Palenik, 1997) or if diurnal changes in the PUB/PEB ratio caused by chromatic adaptation as postulated by Subramaniam et al. (1999).

6 Outlook

The investigations in 2006 and 2007 took place when the Mekong River had its lowest annual discharge. The N_2-fixation rates found contradict the assumption by Voss et al. (2006) that the Mekong River enhances nitrogen fixation only during the south-west monsoon. The investigation in 2007 proofed that the Mekong River has a tremendous influence on its adjacent waters also during the intermonsoon.

It is uncertain, on which scales the examined parameters and processes change during the year and what the influence of the seasonally prevailing monsoon winds is. The much lower salinity during highest discharge in the south-west monsoon and the further offshore reaching river plume should shift the measured activity further off the coast. This could give brackish and freshwater organisms the chance to grow. Additional investigation cruises are necessary to uncover the effects of the Mekong River on abundance and N_2-fixation rates of cyanobacteria within the seasonally changing environment. Vertical distribution of all parameters may be considered for other cruises as well.

It seems undeniable that river water has a huge impact on nitrogen fixation (this study; Carpenter et al., 1999). Unfortunately, already conducted research within river plumes is limited but investigation of N_2-fixation within them could help to diminish the deficit in the global N-budget.

7 Literature

Azam F, Fenchel T, Field JG, Gray JS, Meyer-Reil LA, Thingstad F (1983) The ecological role of water-column microbes in the sea. Marine Ecology Progress Series 10: 257-263

Billard RC, Frensel J (1986) *Rhodella cyanea nov*. sp., une nouvelle Rhodophyceae unicellulaire. Comptes Rendues de l´Académie des Sciences de Paris III 302: 271-276

Breitbarth E, Milliman JD, Friedrichs G, LaRoche J (2004) The Bunsen gas solubility coefficient of ethylene as a function of temperature and salinity and its importance for nitrogen fixation assays. Limnology & Oceanography Methods 2: 282-288

Campbell L (2001) Flow cytometric analysis of autotrophic picoplankton. In: Methods in Microbiology, Vol 30. Academic Press Ltd., p 317-341

Campbell L, Carpenter EJ, Montoya JP, Kustka AB, Capone DG (2005) Picoplankton community structure within and outside a *Trichodesmium* bloom in the southwestern Pacific Ocean. Vie et Milieu 55: 185-195

Campbell L, Vaulot D (1993) Photosynthetic picoplankton community structure in the Subtropical North Pacific Ocean near Hawaii (station ALOHA). Deep-Sea Research I 40: 2043-2060

Capone DG, Burns J, Montoya JP, Subramaniam A, Mahaffey C, Gunderson T, Michaels AF, Carpenter EJ (2005) Nitrogen fixation by *Trichodesmium* spp.: An important source of new nitrogen to the tropical and subtropical North Atlantic Ocean. Global Biogeochemical Cycles 19:GB2024, doi:10.1029/2004GB002331

Capone DG, Subramaniam A, Montoya JP, Voss M, Humborg CJAM, Siefert RL, Carpenter EJ (1998) An extensive bloom of the N_2-fixing cyanobacteria *Trichodesmium erythraeum* in the central Arabian Sea. Marine Ecology Progress Series 172: 281-292

Capone DG, Zehr JP, Paerl H, Bergman B, Carpenter EJ (1997) *Trichodesmium*, a globally significant marine cyanobacterium. Science 276: 1221-1229

Carpenter EJ (1983) Physiology and ecology of marine *Oscillatoria* (*Trichodesmium*). Marine Biology Letters 4: 69-85

Carpenter EJ (2002) Marine cyanobacterial symbioses. Biology and Environment: Proceedings of the Royal Irish Academy 102B: 15-18

Carpenter EJ, Montoya JP, Burns J, Mulholland MR, Subramaniam A, Capone DG (1999) Extensive bloom of a N_2-fixing diatom/cyanobacterial association in the tropical Atlantic Ocean. Marine Ecology Progress Series 185: 273-283

Carpenter EJ, O´Neil JM, Dawaon R, Capone DG, Siddiqui PJA, Ronneberg T, Bergman B (1993) The tropical diazotrophic phytoplankton *Trichodesmium*: Biological characteristics of two common species. Marine Ecology Progress Series 95: 295-304

Chen CA, S. W, B. W, Pai SC (2001) Nutrient budgets for the South China Sea basin. Marine Chemistry 75: 281-300

Chisholm SW, Olson RJ, Zettler ER, Goericke R, Waterbury JB, Welschmeyer NA (1988) A novel free-living prochlorophyte abundant in the oceanic euphotic zone. Nature 334: 340-343

Church MJ, Jenkins BD, Karl DM, Zehr JP (2005) Vertical distributions of nitrogen-fixing phylotypes at Station ALOHA in the oligotrophic North Pacific Ocean. Aquatic Microbial Ecology 38: 3-14

Codespoti LA (2007) An oceanic fixed nitrogen sink exceeding 400 $TgNa^{-1}$ vs. the concept of homeostasis in the fixed-nitrogen inventory. Biogeocsciences 4: 233-253

Colón-López M, Sherman DM, Sherman LA (1997) Transcriptional and translational regulation of nitrogenase in light-dark-and continious-light grown cultures of the unicellular cyanobacterium *Cyanothece* sp. Strain ATCC 51142 Journal of Bacteriology 179: 4319-4327

Dippner JW, Nguyen KV, Hein H, Ohde T, Loick N (2007) Monsoon-Induced upwelling off the Vietnamese Coast. Ocean Dynamics 57: 46-62

Edeler L (1979) Recommondations on methods for marine biological studies in the Baltic Sea. Phytoplankton and Chlorophyll. The Baltic Marine Biologists Publication 5: 1-38

Exton RJ, Houghton WM, Esaias W (1983) Spectral differences and temporal stability of phycoerythrin fluorescence in estuarine and coastal waters due to the domination of lable cryptophytes and stable cyanobacteria. Limnology & Oceanography 28: 1225-1231

Falcón LI, Carpenter EJ, Cipriano F, Bergman B (2004) N_2-Fixation by unicellular bacterioplankton from the Atlantic and Pacific Oceans: phylogeny and in situ rates. Applied and Environmental Microbiology 70: 765-770

Falkowski PG (1997) Evolution of the nitrogen cycle and its influence on the biological sequestration of CO_2 in the ocean. Nature 387: 272-275

Fang G, Fang W, Fang Y, Wang K (1998): A survey of studies on the South China Sea upper ocean circulation. Acta Oceanographica Taiwanica 37: 1-16.

Fang W, Fang G, Shi P, Huang Q, Xie Q (2002) Seasonal structures of upper layer circulation in the southern South china sea from in situ observations. Journal of Geophysical Research 107: 23-21 - 23-12

Foster RA, Subramaniam A, Mahaffey C, Carpenter EJ, Capone DG, Zehr JP (2007) Influence of the Amazon River plume on distribution of free-living and symbiotic cyanobacteria in the western tropical North Atlantic Ocean. Limnology and Oceanography 52: 517-532

French CS, Young VK (1952) The fluorescence spectra of red algae and the transfer of energy from phycoerythrin to phycocyanin and chlorophyll. Journal of General Physiology 35: 873-890

Furuki T, Maeda S, Imajo S, Hiroi T, Amaya T, Hirokawa T, Ito K, Nozawa H (2003) Rapid and selective extraction of phycocyanin from Spirulina platensis with ultrasonic cell disruption. Journal of Applied Phycology 15: 319–324

Gasol JM (1999) How to count picoalgae and bacteria with the FACScalibur flow cytometer. http://www.marbef.org/training/FlowCytometry/Lectures/Gasol2.pdf

Glieskes WWC, Kraay GW (1983) Dominance of Cryptophyceae during the phytoplankton spring bloom in the central North Sea detected by HPLC analysis of pigments. Marine Biology 167: 304-312

Gómez F, Furuya K, Takeda S (2005) Distribution of the cyanobacterium *Richelia intracellularis* as an epiphyte of the Diatom *Chaetoceros compressus* in the western Pacific Ocean. Journal of Plankton Research 27: 323-330

Grasshoff K, Ehrhardt M, Kremling K (1983) Methods of sea water analysis. In. John Wiley, Hoboken, N.J., p 419 pp.

Gruber N, Sarmiento JL (1997) Global patterns of marine nitrogen fixation and denitrification. Global Biogeochemical Cycles 11: 235-266

Hellerman S, Rosenstein M (1983) Normal monthly wind stress over the world ocean with error estimation. Journal of Physical Oceanography 13: 1093-1104

Hoa LTV, Nhan NH, Wolanski E, Cong TT, Shigeko H (2007) The combined impact on the flooding in Vietnam's Mekong River delta of local man-made structures, sea level rise, and dams upstream in the river catchment. Estuarine, Coastal and Shelf Science 71: 110- 116

Holl CM, Montoya JP (2005) Interactions between nitrate uptake and nitrogen fixation in continious cultures of the marine diazotroph *Trichodesmium* (Cyanobacteria). Jounal of Phycology 47: 1178-1183

Hu J, Kawamura H, Hong H, Qi Y (2000) A review on the currents in the South Chiuna Sea: Seasonal circulation, South China Sea Warm Current and Kuroshio Intrusion. Journal of Oceanography 56: 607-624

Jacques G (1968) Aspects qualitatifs du phytoplancton du Banyuls de Mer. 2. Cycle des flagellés nanoplanctoniques. Vie et Milieu 19: 17-35

Janson S, Rai AN, Bergman B (1995) The intracellular symbiont *Richelia intracellularis*: ultrastructure and immuno-localisation of phycoerythrin, nitrogenase, RUBISCO and glutamine synthetase. Marine Biology 124: 1-8

Janson S, Wouters J, Bergman B, Carpenter EJ (1999) Host specificity in the *Richelia*-diatom symbiosis revealed by *hetR* gene sequence analysis. Environmental Biology 1: 431-438

Karl D, Michaels A, Bergman B, Capone DG, Carpenter EJ, Letelier R, Lipschultz F, Paerl H, Sigman D, Stal L (2002) Dinitrogen fixation in the world´s oceans. Biogeochemistry 57/58: 47-98

Langlois RJ, LaRoche J, Raab PA (2005) Diazotrophic diversity and distribution in the tropical and subtropical Atlantic Ocean. Applied and Environmental Microbiology 71: 7910-7919

Lantoine F, Neveux J (1997) Spatial and seasonal variations in abundance and spectral characteristics of phycoerythrins in the tropical northeastern Atlantic Ocean. Deep-Sea Research I 44: 223-246

LaRoche J, Breitbarth E (2005) Importance of the diazotrophs as a source of new nitrogen in the ocean. Journal of Sea Research 53: 67-91

Lepesteur M, Martin JM, Fleury A (1993) A comparative study of different preservation methods for phytoplankton cell analysis by flow cytometry. Marine Ecology Progress Series 93: 55-63

Marie D, Partensky F, Vaulot D, Brussaard C (1999) Enumeration of Phytoplankton, Bacteria, and Viruses in Marine Samples. In: Robinson JP (ed) Current Protocols in Cytometry. John Wiley & Sons Inc., p 11.11.11-11.11.15

Marshall HG (1981) Occurrance of blue-green algae (Cyanophyta) in the phytoplankton of the southeastern coast of the United States. Journal of Plankton Research 3: 163-166

Milliman JDR, C., Meybeck M (1995) River Discharge to the sea: A Global River Index, LOICZ Core Project Office

Mills M, Ridame C, Davey M, LaRoche J, Geider RJ (2004) Iron and phosphorus co-limit nitrogen fixation in the eastern tropical North Atlantic. Nature 429: 292-232

Montoya JP, Holl CM, Zehr JP, Andrew H, Villareal TA, Capone DG (2004) High rates of N_2 fixation by unicellular diazotrophes in the oligotrophic Pacific Ocean. Nature 430: 1027-1031

Montoya JP, Voss M, Kähler P, Capone DG (1996) A simple, high-precision, high-sensitive tracer assay for N_2 fixation. Applied and Environmental Microbiology 62: 986-993

Moreth CM, Yentsch CS (1970) A sensitive Method for the determination of open ocean phytoplankton phycoerythrin pigments by fluorescence. Limnology & Oceanography 15: 313-317

Mulholland MR, Capone DG (2001) The stoichometry of N and C utilization in cultured populations of *Trichodesmium* IMS101. Limnology & Oceanography 46: 436-443

Neveux J, Lantoine F, Vaulot D, Marie D, Blanchot J (1999) Phycoerythrins in the southern tropical and equatorial Pacific Ocean: Evidence for new cyanobacterial types. Journal of Geophysical Research 104: 3311-3321

Neveux J, Tenorio MMB, Cecile D, Villareal TA (2006) Spectral diversity of phycoerythrins and diazotroph abundance in tropical waters. Limnology & Oceanography 51: 1689-1698

Nittrouer CA, Brunskill GJ, Figueiredo AG (1995) Importance of tropical coastal environments. Geo-Marine Letters 15: 121-126

Olson RJ, Chisholm SW, Zettler ER, Ambrust EV (1988) Analysis of *Synechococcus* pigment types in the sea using single and dual beam flow cytometry. Deep-Sea Research Part A 35: 425-440

Olson RJ, Chisholm SW, Zettler ER, Ambrust EV (1990) Pigment, size and distribution of *Synechococcus* in the North Atlantic and Pacific Ocean. Limnology & Oceanography 35: 45-58

Rueter JG (1988) iron stimulation of photosynthesis and nitrogen fixation in *Anabena* 7120 and *Trichodesmium* (Cyanophyceae). Journal of Phycology 24: 1245-1248

Saito Y (2001) Deltas in Southeast and East Asia: Their evolution and current problems Global change in Asia Pacific Coast - Proceedings of Asien-Pacific Network for Global Change Research

Sigman DM, Casciotti KL (2001) Nitrogen Isotopes in the ocean. In: Encyclopedia of Ocean Sciences, p 1884-1894, doi: 10.1006/rwos2001.0172

Staal M, Meysman FJR, Stal L (2003) Temperature excludes N_2-fixing heterocysteous cyanobacteria in the tropical oceans. Nature 425: 504-507

Subramaniam A, Carpenter EJ, Karentz D, Falkowski PG (1999) Bio-optical properties of the marine diazotrophic cyanobacteria *Trichodesmium* spp. I: Absorption and photosynthetic action spectra. Limnology & Oceanography 44: 608-617

Toledo G, Palenik B (1997) *Synechococcus* diversity in the California Current as seen by RNA polymerase (*rpoC1*) gene sequences of isolate strains. Applied and Environmental Microbiology 63: 4298-4303

Utermöhl vH (1958) Zur Vervollkommnung der quantitativen Phytoplankton-Methodik. Mitt. Int. Verein. Theor. Angew. Limnol. 9: 1-38

Villareal TA (1992) Marine nitrogen-fixing diatom-cyanobacteria symbioses. In: Carpenter EJ, Capone DG, Rueter JG (eds) Marine pelagic cyanobacteria: *Trichodesmium* and other diazotrophes. Kluwer, Dordrecht, p 163-174

Viskari PJ, Colyer CL (2003) Rapid extraction of phycobiliproteins from cultured cyanobacteria samples. Analytical Biochemistry 319: 263-271

Voss M, Bombar D, Loick N, Dippner J (2006) Riverine influence on nitrogen fixation in the upwelling region off Vietnam, South China Sea. Geophysical Research Letters 33: L07604, doi:10.29/2005GL025569

Voss M, Croot P, Lochte K, Mills M, Peeken I (2004) Patterns of nitrogen fixation along 10°N in the tropical Atlantic. Geophysical Research Letters 31: L23S09; doi:10.1029/2004GL020127

Walsby AE (1991) The gas vesicles and buoyancy of *Trichodesmium*. In: Carpenter EJ, Capone DG, Rueter JG (eds) Marine Pelagic Cyanobacteria: *Trichodesmium* and other Diazotrophs. Kluwer Dordrecht, p 141-163

Wu J, Chung S-W, Wen L-S, Liu K-K, Chen Y-LL, Chen H-Y, Karl D (2003) Dissolved inorganic phosphorus, dissolved iron, and *Trichodesmium* in the oligotrophic South China Sea. Global Biogeochemical Cycles 17: 1008; doi:1010.1029/2002GB001924

Wyman M (1992) An in vivo method for the estimation of phycoerythrin concentrations in marine cyanobacteria (*Synechococcus* spp.). Limnology & Oceanography 37: 1300-1306

Zehr JP, Mellon MT, Zani S (1998) New nitrogen fixing microorganisms detected in oligotrophic oceans by amplification of nitrogenase (*nifH*) genes. Applied and Environmental Microbiology 64: 3444-3450

Zehr JP, Montoya JP, Jenkins BD, Hewson I, Mondragon E, Short CM, Church MJ, Andrew H, Karl DM (2007) Experiments linking nitrogen gene expression and nitrogen fixation in the North Pacific subtropical gyre. Limnology and Oceanography 52: 169-183

Zehr JP, Waterbury JB, Turner PJ, Montoya JP, Enoma O, Steward GF, Andrew H, Karl DM (2001) Unicellular cyanobacteria fix N_2 in the subtropical North Pacific Ocean. Nature 412: 635-638

8 Acknowledgments

I would like to thank all the people that made this thesis possible and an enjoyable experience for me

I am deeply indebted to my supervisor Maren Voß for her constant support and the opportunity to experience the Vietnamese Way of Life first hand.

I am greatful to Iris Liskow and Annett Grüttmüller for their support in the lab, and to the phytoplankton-group at the ION for counting my endless samples.

Furthermore, I would like to thank Nicola Wannicke, the “Arbeitsgruppe Ökologie” and Jacques Neveux for their assistance in establishing the phycoerythrin measurements.

I would also like to thank the people in Office 100 for the long-lasting discussions and the endless supply of coffee.

I would also like to acknowledge my office mates for all the great laughs and the funny time.

Finally I would like to thank my family for their constant support, understanding and love.

9 Appendix

I. List of tables

II. List of figures

Selbständigkeitserklärung

Hiermit versichere ich, dass ich die vorliegende Arbeit selbständig verfasst und keine anderen als die angegebenen Quellen (siehe § 25, Abs. 7 der Diplomprüfungsordnung Biologie 2000) und Hilfsmittel verwendet habe.
Mir ist bekannt, dass gemäß § 8, Abs. 3 der Diplomprüfungsordnung Biologie 2000 die Prüfung wegen einer Pflichtwidrigkeit (Täuschung u.ä.) für nicht bestanden erklärt werden kann.

Rostock, den 22.Oktober 2007

Julia Große